JOURNAL OF QUATERNARY SCIENCE (2025) **40**(4) 604–621 ISSN 0267-8179. DOI: 10.1002/jqs.3699

JQS Journal of Quaternary Science QRA Quaternary Research Association

Restricted cirque glaciers in the Wicklow Mountains, Ireland, during the Nahanagan Stadial (Greenland Stadial-1/Younger Dryas)

LAUREN KNIGHT,[1] CLARE M. BOSTON,[1] HAROLD LOVELL,[1]* TIMOTHY T. BARROWS,[2] ERIC A. COLHOUN,[3] DAVID FINK[4] and NICHOLAS C. PEPIN[1]

[1]School of the Environment and Life Sciences, University of Portsmouth, Portsmouth, UK
[2]Chronos Radiocarbon Facility, UNSW Sydney, Sydney, NSW, Australia
[3]School of Environmental and Life Sciences, University of Newcastle, Newcastle, NSW, Australia
[4]Australian Nuclear Science and Technology Organisation (ANSTO), Sydney, NSW, Australia

Received 14 October 2024; Revised 28 January 2025; Accepted 5 February 2025

ABSTRACT: In Ireland, the Nahanagan Stadial (NS) was characterised by cirque glacier, plateau icefield and mountain ice cap expansion and is named after the cirque glacier type-site of Lough Nahanagan in the Wicklow Mountains. This period is broadly equivalent to the Younger Dryas Stadial and Greenland Stadial-1 (GS-1: ~12.9–11.7 ka). Here, we provide the first evaluation of the full extent of NS glaciation in the Wicklow Mountains by combining solar radiation modelling, mapping of glacial geomorphology, ^{10}Be and ^{26}Al cosmogenic surface exposure dating, 3D glacier reconstructions and analysis of snowblow and avalanching potential. We identify seven sites that hosted cirque glaciers at this time. Glacier extent was very restricted, with most glaciers only partially filling their cirques. Equilibrium line altitudes (ELAs) ranged from 470 ± 5 m a.s.l. (Lough Nahanagan) to 721 ± 5 m a.s.l. (Lough Cleevaun), with an average ELA of 599 m a.s.l. Higher snowblow and avalanching contributions at sites with lower ELAs demonstrate local topoclimatic influence on glacier growth and preservation alongside regional climate. The Wicklow Mountains provides a good example of marginal cirque glaciation during GS-1 and the importance of local topography and microclimate for sustaining glaciers in some mountain areas of Britain and Ireland.

KEYWORDS: cirque glaciation; Greenland Stadial-1; Ireland; Nahanagan Stadial; surface exposure dating

Introduction

Greenland Stadial-1 (GS-1: ~12.9–11.7 ka; Rasmussen et al., 2014) was a period of rapid climate cooling in the North Atlantic region when ice masses advanced in mountainous areas of Britain and Ireland (Barr et al., 2017b; Barth et al., 2018; Bickerdike et al., 2018). Reconstructions of glaciers that formed during this period provide important information on local and regional palaeoclimate during the Late Quaternary (e.g., Benn and Ballantyne, 2005; Lukas and Bradwell, 2010; Finlayson et al., 2011; Boston et al., 2015; Chandler et al., 2019). This is valuable for building knowledge on the environmental response to rapid climatic change in this region.

In Ireland, the Nahanagan Stadial (NS) is considered the regional expression of GS-1, equivalent to the Loch Lomond Stadial (LLS) in Britain (Bickerdike et al., 2018), and is based on the type-site at Lough Nahanagan in the Wicklow Mountains. Here, a small cirque glacier left a series of moraines within the confines of the lough, dated to 13 165–10 144 cal a BP and 12 111–11 041 cal a BP (Colhoun and Synge, 1980; calibrated from 11 500 ± 550 ^{14}C a BP and 11 600 ± 260 ^{14}C a BP, respectively, using IntCal20, Reimer et al., 2020). Elsewhere in Ireland, cirque glaciation of a similar scale has been identified at Macgillycuddy's Reeks in the southwest (Anderson et al., 1998; Harrison et al., 2010), the Derryveagh Mountains in the northwest (Wilson, 2004) and the Mourne Mountains in the northeast (Barr et al., 2017a). Cirque glaciation has also been reconstructed eastwards across the Irish Sea in Eryri (also known as Snowdonia; Bendle and Glasser, 2012) and Bannau Brycheiniog (also known as Brecon Beacons; Coleman and Carr, 2008).

The next best constrained evidence for NS glaciation in the Wicklow Mountains after Lough Nahanagan is found at Kelly's Lough (Leira et al., 2007; Barth et al., 2018). Tomkins et al. (2018) argued for NS ice at two further sites (Upper Lough Bray and Mullaghcleevaun) based on Schmidt hammer exposure dating (SHED) and concluded that snow redistribution and local topographic controls were likely key components of glacier survival during the NS. There is also geomorphological evidence for small ice masses at several other sites (Knight et al., 2023), but a full investigation of NS glacier extent has yet to be undertaken. Here, we (1) identify potential NS glacier-hosting sites based on solar radiation modelling, mapping of glacial geomorphology and ^{10}Be and ^{26}Al cosmogenic surface exposure ages and (2) reconstruct former glacier size and equilibrium line altitudes (ELAs), including an assessment of regional palaeoclimate and the influence of wind-driven snow redistribution and avalanching on glacier accumulation areas.

Study area and glacial history

The Wicklow Mountains are located in eastern Ireland, about 20 km inland from the Irish Sea coast. The mountains consist of plateaux with rounded peaks, including the highest point of Lugnaquillia (925 m above sea-level (a.s.l.)) in the south (Fig. 1). The dominant lithology is granite with mica-schist exposed in

*Correspondence: Harold Lovell, as above.
Email: harold.lovell@port.ac.uk

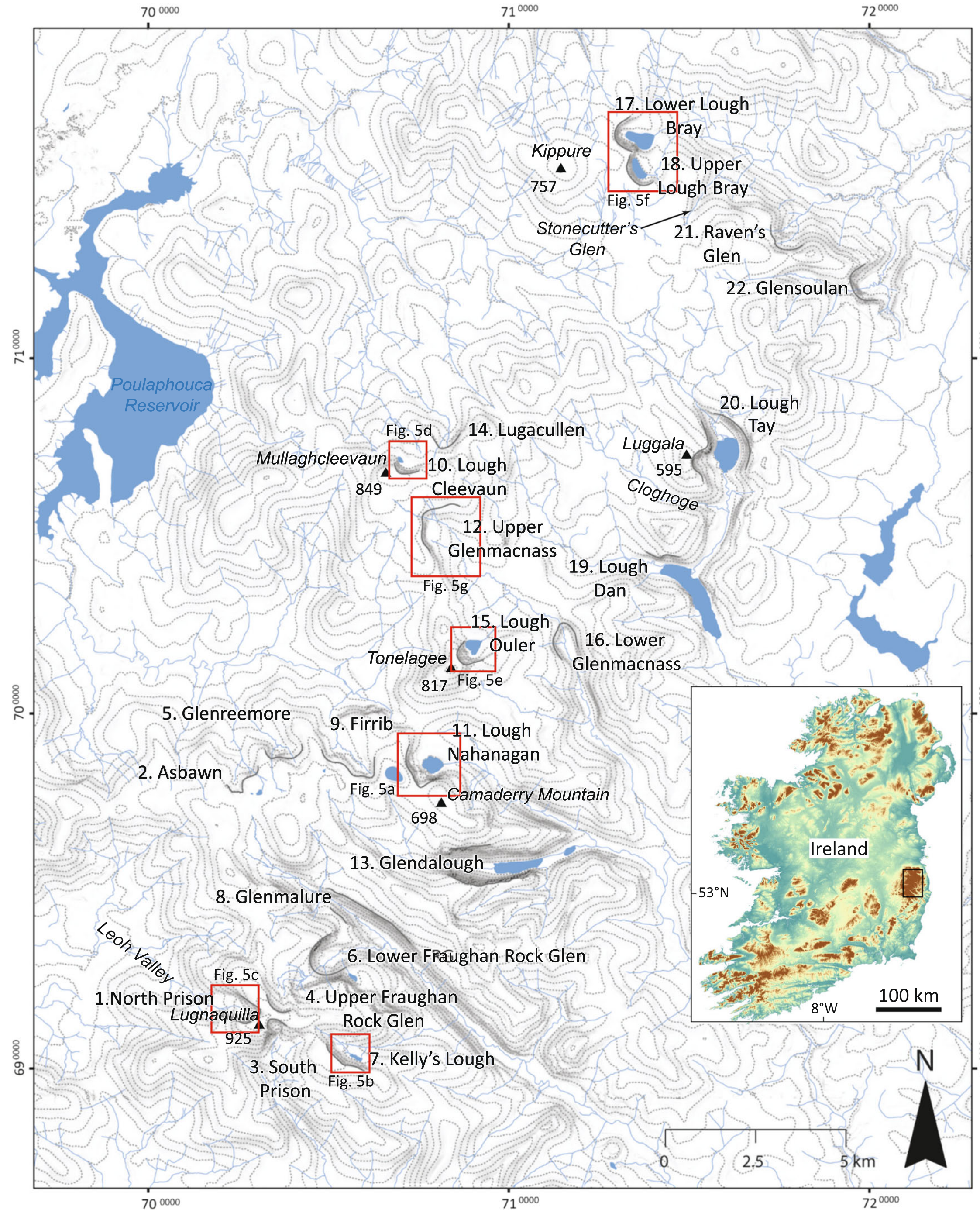

Figure 1. Location map of the Wicklow Mountains showing major peaks and 22 possible Nahanagan Stadial glacier-hosting sites. Sites are numbered from west to east. See Table S1 for further details on each site. Red boxes show the locations of the detailed geomorphological maps in Fig. 5. The grid reference is Irish Transverse Mercator (units: metres). The inset map shows the study area (black rectangle) within Ireland shown on a relief-shaded elevation model derived from SRTM data (spatial resolution: 30 m). [Color figure can be viewed at wileyonlinelibrary.com]

places, with the geological boundary between the two controlling the location of glacial overdeepenings at Glendalough, Glenmacnass and Lough Tay (Coxon et al., 2012).

At the local last glacial maximum (LLGM) in Britain and Ireland, the maximum extent of the British–Irish Ice Sheet was reached at ~30–22 ka in different sectors, and the maximum ice volume occurred at ~23 ka (Clark et al., 2022). The Wicklow Mountains hosted an independent ice dome within the British–Irish Ice Sheet during the LLGM that covered all but the highest peaks and was coalescent with terrestrial ice and the Irish Sea Ice Stream (Ballantyne et al., 2006; Clerc et al., 2012). Glaciated peaks became ice free after ~21 ka based on ^{10}Be exposure ages (Ballantyne et al., 2006; recalculated by Tomkins et al., 2018). The ice dome fragmented and transitioned to a phase of alpine-style glaciation that persisted until ~15.4 ka, characterised by switches between stable margin positions and readvances of large valley glaciers fed by summit icefields (Warren, 1993; Tomkins et al., 2018).

There are a number of topographic hollows with the potential to host glaciers in a restricted phase of glaciation such as the NS, including cirques, overdeepenings and strongly defined valley heads (Fig. 1). NS glacier expansion in the Wicklow Mountains was previously suggested to be restricted to cirques >350 m a.s.l. (Colhoun and Synge, 1980).

At Lough Nahanagan (400 m a.s.l.) (Fig. 1), Colhoun and Synge (1980) mapped 13 inner cirque moraine ridges exposed on the lake bed in 1968 CE when the water level was lowered ~40 m during hydroelectric works. The moraine ridges are typically <5 m high, narrow, sharp-crested and, although discontinuous, can be traced across the width of the cirque. Moraine internal structure suggests that most were formed subaqueously within a glacial lake dammed between the cirque glacier margin and the much larger, broad and rounded outer cirque moraine (Colhoun and Synge, 1980). Organic material found within glaciotectonised lake clays exposed within two of the subaqueous moraine ridges located furthest from the backwall returned ^{14}C ages of 13 165–10 144 cal a BP and 12 111–11 041 cal a BP (Colhoun and Synge, 1980). A boulder on the outer cirque moraine has a ^{36}Cl exposure age of 22.4 ± 1.3 ka (Bowen et al., 2002; recalculated from 17.9 ± 1.0 ka; see further details in Methods and Table S3). This same outer moraine has also been dated using SHED to 10.9 ± 0.3 ka by Tomkins et al. (2018), who explained this large discrepancy compared to the ^{36}Cl and ^{14}C chronology as possibly relating to uncertainties introduced by predepositional and/or postdepositional processes. Together, the simplest interpretation of the moraine sequences at Lough Nahanagan is that the outer cirque moraine (large, broad and rounded) was deposited by a glacier readvance or stillstand at ~22.4 ka during overall retreat following the LLGM and the series of inner cirque moraines were deposited during the NS sometime between 13 and 10 ka (Colhoun and Synge, 1980; Bowen et al., 2002).

The second site where a NS-age glacier has been identified is Kelly's Lough (587 m a.s.l.) (Fig. 1). Here, a suite of small, bouldery moraines have been mapped (Knight et al., 2023), ^{10}Be exposure dated to 10.8 ± 0.5 ka (Barth et al., 2018) and SHED dated to 12.0 ± 0.4 ka (Tomkins et al., 2018). Additionally, a core taken from Kelly's Lough returned a basal age of 11 160–10 750 cal a BP, supporting glacial occupation of the lough during the NS (Leira et al., 2007).

Suites of moraines of a similar size, morphology and distribution to those at Lough Nahanagan and Kelly's Lough have been mapped within several other cirques (Knight et al., 2023) and NS ages have been reported by Tomkins et al. (2018) from two other sites using the SHED technique: Upper Lough Bray (12.3 ± 0.5 ka) and Mullaghcleevaun (11.4 ± 0.1 ka; hereafter, we use Upper Glenmacnass for this site) (Fig. 1). In addition, at Upper Lough Bray, Bowen et al. (2002) obtained a ^{36}Cl exposure age of 14.3 ± 1.0 ka (recalculated from 15.7 ± 1.1 ka; see further details in Methods and Table S3).

Methods

Solar radiation modelling

Incoming solar radiation is the dominant source of melt energy on most glaciers (Olson and Rupper, 2019). Solar radiation modelling was used to assess the relative radiation receipt in the Wicklow Mountains to identify sites with enhanced topographic shading that may have hosted NS glaciers. We used the Solar Analyst model in Esri ArcGIS 10.4 (e.g., Zhang et al., 2015) and a digital terrain model (DTM) from Ordnance Survey Ireland (OSI; spatial resolution: 10 m) to calculate the accumulated incoming short-wave solar radiation receipt at each grid cell based on 1 day each month (calculated in increments of 30 days before and after the summer solstice on 21 June). These 12 days, representative of each month of the year, were summed over a calendar year to obtain an annual total (in watt-h per m^2; $Wh\,m^{-2}$).

Geomorphological mapping and relative chronology assessment

The glacial geomorphology in the Wicklow Mountains is presented in detail in Knight et al. (2023). Here, the focus is on the geomorphology located within sites that potentially hosted NS glaciers. Glacial, periglacial and fluvial sediment–landform assemblages were mapped in the field at a scale of 1:10 000 and in Esri ArcGIS using a DTM (spatial resolution: 10 m) and orthorectified aerial photographs from OSI (spatial resolution: 1 m) following standard approaches (Chandler et al., 2018). We used morphostratigraphic principles to identify and separate glacial events into a relative chronology. This approach examines variations in individual landform characteristics and the spatial relationship between suites of different landforms (e.g., moraines, meltwater channels and river terraces) to develop a relative sequence of glacial events and establish a geochronological framework (Lukas, 2006).

Surface exposure dating

Rock samples were collected from the top of prominent boulders on moraines at Kelly's Lough, Upper Lough Bray, Lower Lough Bray and Lough Tay (Fig. 1 and Table S2). Both multiple boulders on a single moraine (at Upper Lough Bray) and individual boulders on different moraines (all sites) were sampled. Horizon shielding was measured by using a clinometer in the field. All calculated exposure ages are based on zero erosion, as there are no independent data for the local lithology by which to make a reliable erosion-corrected exposure age. However, given that all ages range between 30 and 10 ka, using an assumed erosion rate typical for similar lithologies of 5 mm ka^{-1} would incur no more than a 5% increase in exposure age across this age range. In addition, corrections for winter snow shielding are not included due to an absence of long-term historical data that are required to extrapolate snow shielding corrections over the past 10–30 ka.

Beryllium-10 and ^{26}Al Accelerator Mass Spectrometry (AMS) measurements were performed at ANSTO (Australian Nuclear Science and Technology Organisation; Fink et al., 2004) on the 10MV ANTARES AMS facility following methods reported in Fink and Smith (2007). Where more than one isotope was measured, ages were combined as weighted means, with external error as the uncertainty and the production rate uncertainty added in quadrature. All accepted ages (be they deduced from single- or dual-isotope ages) from boulders on the same moraine, or boulders from separate moraines at the same site that are deemed to have formed coevally, were statistically combined (using weighted means and errors) to provide a best estimate of the landform age. All ages were calculated using the CRONUS-Earth online exposure age calculator v3 (http://hess.ess.washington.edu/math/), the LSDn scaling scheme (Lifton et al., 2014), the primary calibration data set of Borchers et al. (2016) and a rock density of 2.7 g cm^{-3}. Further details on sample preparation, AMS measurements and age calculations can be found in the Supporting Information.

Recalculation of previously published exposure ages

Two ^{36}Cl exposure ages from the Wicklow Mountains were recalculated from Bowen et al. (2002) (Tables S3 and S4). Elevation was determined using the 10 m DTM. A measurement error of 2% was ascribed to major elements (>10%), 5% to minor elements (<10%) and 10% to trace elements. The major, minor and trace element composition was normalised to 100%, assuming 1% ± 50% analytical water. Ages were calculated using CRONUScalc version 2.0 (Marrero et al., 2016) and were scaled using the SA scheme of Lifton et al. (2014).

Glacier reconstruction and ELA calculations

Three-dimensional (3D) glacier reconstruction was carried out for sites identified as likely to have hosted NS glaciers through a combination of glacier surface profile modelling and manually digitised glacier reconstruction (e.g., Boston et al., 2015; Chandler and Lukas, 2017; Chandler et al., 2019). Surface profile modelling using the Benn and Hulton (2010) 'perfectly plastic' flowline model was used to constrain glaciologically plausible ice thicknesses in the upper part of the cirques where geomorphological evidence is lacking. Profile modelling was used to identify the likely area of glacier–backwall interception and to model ice thickness along the central flowline. The only existing cirque lough depth data are from Kelly's Lough, measured at 8 m (Leira et al., 2007). Based on these, small loughs were given approximate depths of ~8 m, whereas larger loughs were given approximate depths of up to 20 m. The elevations of latero-frontal moraines, where present, were used as 'target elevations' to guide ice thickness. A yield stress of ~50 kPa was used where possible following Chandler and Lukas (2017), but 20 kPa had to be used to fit some target latero-frontal moraines. Yield stresses of similar magnitude to those in the geomorphologically constrained parts of the glaciers were used to extrapolate the former glacier surface into unconstrained areas and yield stress was increased in association with any steepening slopes, such as at the backwall (Benn and Hulton, 2010; Boston et al., 2015).

The ELA is defined as the altitude where net annual accumulation and ablation are equal. It is primarily controlled by the balance between temperature and precipitation (Ohmura et al., 1992), and thus can be used to derive palaeoclimate information from glacier reconstructions. We used two methods for ELA calculation: the accumulation-area ratio (AAR) and the area–altitude balance ratio (AABR).

The AABR is considered the most reliable ELA calculation method for the majority of palaeoglaciological situations (Rea, 2009; Pellitero et al., 2015; Oien et al., 2022), since it accounts for glacier hypsometry and uses a balance ratio to include different accumulation and ablation gradients. However, it assumes that (1) accumulation and ablation gradients are approximately linear; (2) the ratio between these two gradients remains fixed over time; and (3) topography constrains an ice mass to a sufficient extent that changes to mass balance manifest as a change to terminus position (advance or retreat).

Based on modern glacier data, Rea (2009) suggested that a balance ratio of 1.9 ± 0.81 is most appropriate for mid-latitude maritime glacier reconstructions and this value has been adopted by most subsequent studies (e.g., Boston et al., 2015; Barr et al., 2017b; Chandler and Lukas, 2017; Chandler et al., 2019). A more recent comparison of calculated ELAs and measured ELAs from field observations demonstrated that the global median AABR value of 1.56 provided the closest estimates to measured ELAs (Oien et al., 2022), and we therefore use this value too. We also calculated ELAs using AABRs of 1.67, 1.8 and 2.0 for comparability with previous studies (e.g., Benn and Ballantyne, 2005; Lukas and Bradwell, 2010). Similarly, we also used the AAR for comparison with other studies, which is based on contemporary glacier measurements and assumes that a glacier's accumulation area occupies a fixed proportion of the total glacier area. We used AARs of 0.5 and 0.6, meaning that 50% or 60% of the glacier area is in the accumulation zone. These values are deemed the most representative of mid-latitude glaciers without significant debris cover (Benn and Ballantyne, 2005).

Following Pellitero et al. (2015), we added a ±5 m maximum error to all ELAs, which is half of the 10 m contour interval used in the ELA calculations. The exception to this is the ELA calculations carried out using the 1.9 ± 0.81 AABR. Here, we calculated ELA errors using the lower and upper AABRs based on the ±0.81 uncertainty (e.g., 1.09 and 2.71, respectively) and report this figure instead if it is greater than ±5 m.

Palaeoprecipitation calculations

The empirical relationship between temperature and precipitation at glacier ELAs is well established (e.g., Ohmura et al., 1992; Ohmura and Boettcher, 2018, and references therein). Based on this relationship, palaeoprecipitation totals can be estimated at reconstructed glacier ELAs if an independent proxy for summer temperatures is available (Benn and Ballantyne, 2005). Here, palaeoprecipitation values were calculated using the equation formulated by Ohmura et al. (1992) to describe the temperature–precipitation relationship. This method is deemed appropriate for palaeoprecipitation reconstruction in the Wicklow Mountains, as the equation is derived from the examination of 70 mid-latitude and high-latitude contemporary glaciers in localities arguably comparable to eastern Ireland during the NS, including Scandinavia and Iceland.

The relationship between temperature and precipitation is described by Ohmura et al. (1992) as

$$P_a = 645 + 296T_3 + 9T_3^2$$

where P_a is the annual precipitation (mm a^{-1}) and T_3 is the mean summer (3 months) temperature (°C) at the ELA. Ohmura et al. (1992) suggested that a standard error of ±200 mm a^{-1} is included to account for differences in the relationship between air temperature and ablation.

An independent proxy for the mean temperature of the warmest month (July) is needed to calculate precipitation. We used coleopteran assemblage data from Ballybetagh Bog, ~7 km northeast of the Wicklow Mountains, which yielded a calibrated median value for a NS July temperature of 9°C at 230 m a.s.l. (Coope et al., 1998). This was converted into a July temperature at sea level of 10.38°C–10.61°C using typical moist adiabatic lapse rates of 0.006°C–0.007°C m^{-1} (Ballantyne, 2002), equating to a best estimate mean July temperature at sea level of 10.495°C. The Ohmura et al. (1992) calculation requires the mean July temperature (at sea level) to be transformed into a mean summer temperature (at sea level). Here, we use a sinusoidal function from Hofmann et al. (2024):

$$T_3 = T_{\text{mean}} + \frac{\frac{\delta T}{\frac{12}{\pi} \times \sin\left(\frac{\pi}{12}\right)}}{2} \times \frac{12}{3\pi} \times \sin\left(\frac{3\pi}{12}\right)$$

where T_{mean} is the mean annual temperature and δT is the annual temperature range (°C). This can be simplified as follows:

$$T_3 = T_{\text{mean}} + \frac{\delta T}{6} \times \frac{\sin\left(\frac{3\pi}{12}\right)}{\sin\left(\frac{\pi}{12}\right)}$$

To derive T_{mean}, we used:

$$T_{mean} = \frac{T_{January} + T_{July}}{2} = T_{July} - \frac{\delta T}{2}$$

where T_{July} is the mean July temperature and $T_{January}$ is the mean January temperature. Inputting a δT of 34°C (Isarin et al., 1998) and a T_{July} of 10.495°C into the above equations yields a T_3 at sea level of 9.156°C. Using an average lapse rate of −0.0065°C m^{-1}, T_3 was transformed into the average summer temperature at the ELA (1.56 AABR) of each reconstructed glacier. T_3 at the ELA was then used to calculate precipitation for each glacier. In addition to the ±200 mm a^{-1} standard error (Ohmura et al., 1992), the lower boundary of uncertainty (minimum precipitation) was calculated using the lower adiabatic lapse rate (0.006°C m^{-1}) to convert T_{July} into sea level and the upper adiabatic lapse rate (0.007°C m^{-1}) to convert T_3 from sea level into the +5 m ELA (to include the ELA standard error). Conversely, the upper boundary of uncertainty (maximum precipitation) was calculated using the upper adiabatic lapse rate (0.007°C m^{-1}) to convert the T_{July} into sea level and the lower adiabatic lapse rate (0.006°C m^{-1}) to convert T_3 from sea level into the −5 m ELA (to include the ELA standard error).

We also calculated precipitation values at sea level in order to be able to compare the results with other studies. Ballantyne (2002) suggested the following equation to describe changes in precipitation with altitude:

$$P_{Z1} = P_{Z2}/(1 + P^*)^{0.01(Z2-Z1)}$$

where P_{Z1} and P_{Z2} are precipitation totals (mm a^{-1}) at sea level and the ELA, respectively. P^* is the proportional increase in precipitation per 100 m increase in elevation. In the absence of other data, here we use $P^* = 0.0578$, derived by Ballantyne (2002) from a data set for Ben Nevis, Scotland.

Modelling snowblow and avalanche potential

For small glaciers, non-climatic factors such as enhanced snow accumulation from windblown snow and avalanching can exert a strong influence on ELAs (e.g., Benn and Ballantyne, 2005; Coleman et al., 2009; DeBeer and Sharp, 2009; Mills et al., 2009; Bendle and Glasser, 2012; Chandler and Lukas, 2017) and sustain glaciers below the regional ELA (Mitchell, 1996; Lie et al., 2003; Hughes, 2010; Mills et al., 2019; Hofmann et al., 2024). Glacier accumulation can be enhanced by windblown snow sourced from all ground lying above and sloping towards the glacier (Sissons and Sutherland, 1976) and by snow avalanching from steep slopes above the glacier (Mitchell, 1996).

To examine the potential for windblown snow, 'snowblow', at each site, potential snowblow areas (PSBAs) and potential avalanche areas (PAAs) were manually digitised for all reconstructed glaciers using a DTM-derived slope model. PSBAs are defined as all ground lying above the ELA and laterally continuous to the glacier including plateau surfaces (Mitchell, 1996). Snow can be blown uphill, but steep uphill slopes may act as snow fences, blocking snow movement (Robertson, 1989; Coleman et al., 2009; Chandler and Lukas, 2017). Therefore, a maximum slope angle of 10° for slopes dipping away from each glacier was used as the threshold for viable windblown snow (Mitchell, 1996). It is worth noting, however, that Humlum (2002) argues that upslope movement of snow is often underestimated, and therefore, these snowblow calculations should be considered conservative. PAAs are defined as areas sloping towards the glacier that exceed 20° (Sissons and Sutherland, 1976; Chandler and Lukas, 2017).

To assess potential snowblow and avalanching from different wind directions, qualifying areas were divided into 15° sectors and drawn as polar plots. PSBAs and PAAs can be expressed as snowblow and avalanche ratios, calculated as the ratio of potential snowblow/avalanche area to glacier area. However, within each PSBA or PAA, areas further away from the glacier will contribute less to the glacier than areas closer, and the snowblow or avalanche ratios do not account for this. Therefore, Sissons (1980) suggested using snowblow and avalanche factors, which are calculated by taking the square root of the snowblow ratio or avalanche ratio, respectively.

Results

Possible Nahanagan Stadial glacier-hosting sites

We identify 22 possible NS glacier-hosting sites, characterised as topographic hollows with the potential to accumulate snow and provide shading, including cirques, overdeepenings and strongly defined valley heads (Fig. 1 and Table S1). Here, we describe in turn the three key data sets used to assess the likelihood that a site hosted a glacier during the NS: (1) solar radiation modelling (Figs. 2 and 3); (2) geomorphological evidence and morphostratigraphical analysis (Figs. 4 and 5); and (3) surface exposure ages (Fig. 6 and Table 1). Each approach is first considered independently before we perform a combined and considered assessment of likely NS glacier-hosting sites based on all of the available evidence.

Solar radiation modelling

There are clear differences in radiation received at different sites (Figs. 2 and 3). For example, on 21 June (summer solstice; Julian Day 172), high radiation receipts of 6371 Wh m^{-2} and 6178 Wh m^{-2} are modelled at Upper Glenmacnass (12) and the South Prison (3), respectively (Figs. 2 and 3a). In contrast, radiation at Lough Ouler (15) and Lough Nahanagan (11) is significantly lower at 3077 Wh m^{-2} and 3548 Wh m^{-2}, respectively. Average accumulated radiation during the ablation season (estimated as the average of the 6 chosen days from April to September inclusive) is categorised as medium below 3000 Wh m^{-2} and low below 1500 Wh m^{-2}, with Lough Nahanagan (11), Lough Ouler (15) and North Prison (1) fitting between these illustrative thresholds (Fig. 3b).

Upper Glenmacnass (12), which Tomkins et al. (2018) suggest hosted a NS glacier, has the highest levels of modelled average ablation season radiation (Fig. 3b). This value is for the whole cirque, however, whereas the positioning of moraines in Upper Glenmacnass (Knight et al., 2023) (Fig. 5g) suggests that ice would largely have been shaded beneath the western valley flank (Fig. 2). Other sites previously identified as hosting NS glaciers (Lough Nahanagan (11) and Kelly's Lough (7)) have between low and medium average radiation levels during the ablation season (Fig. 3b). Similar to Upper Glenmacnass (12), the configuration of moraines in Kelly's Lough (7) (Fig. 5b) indicates glacier ice residing below the southwestern flank of a larger cirque, which would again reduce the average radiation values here. Based on this analysis, other sites of interest that have higher levels of shading include Lough Ouler (15), North Prison (1), Upper Lough Bray (18), Lower Lough Bray (17),

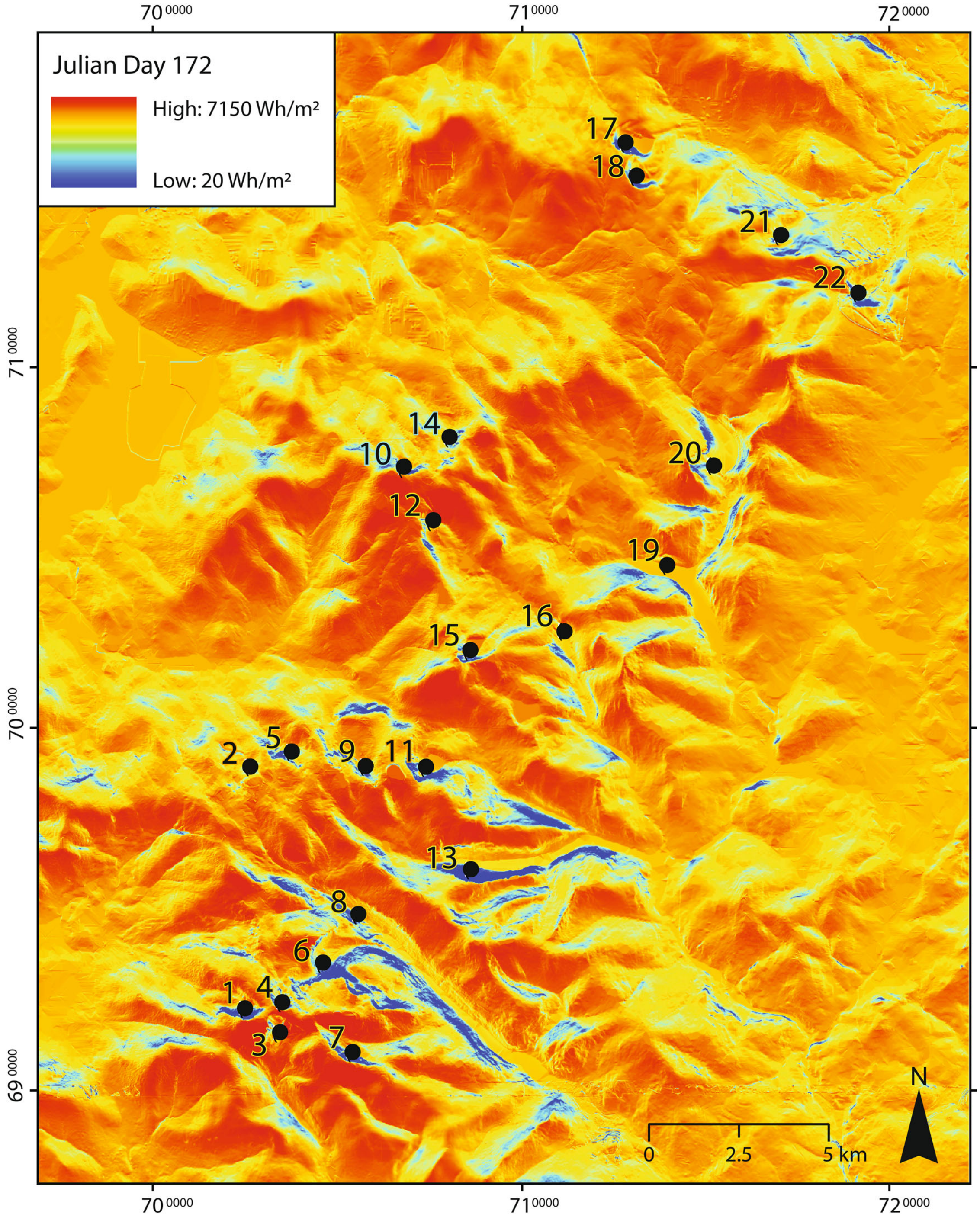

Figure 2. Modelled accumulated incoming solar radiation (over 24 h) at the summer solstice on 21 June (Julian Day 172). Numbered locations: (1) North Prison, (2) Asbawn, (3) South Prison, (4) Upper Fraughan Rock Glen, (5) Glenreeemore, (6) Lower Fraughan Rock Glen, (7) Kelly's Lough, (8) Glenmalure, (9) Firrib, (10) Lough Cleevaun, (11) Lough Nahanagan, (12) Upper Glenmacnass, (13) Glendalough, (14) Lugacullen, (15) Lough Ouler, (16) Lower Glenmacnass, (17) Lower Lough Bray, (18) Upper Lough Bray, (19) Lough Dan, (20) Lough Tay, (21) Raven's Glen, and (22) Glensoulan. The grid reference is Irish Transverse Mercator (units: metres). [Color figure can be viewed at wileyonlinelibrary.com]

Lough Cleevaun (10), Glendalough (13) and Lower Fraughan Rock Glen (6) (Figs. 2 and 3).

Geomorphological evidence and morphostratigraphical analysis

Moraines occur sporadically across the Wicklow Mountains (Knight et al., 2023). The number and size of these moraines are generally low compared to similar upland regions elsewhere in Ireland (cf. Mourne Mountains; Barr et al., 2017b) and Scotland (cf. Bickerdike et al., 2018). We divide the moraines into three classes based on their morphological characteristics and general composition (Fig. 4). Class 1 moraines are large (>10 m height), broad-crested and highly vegetated ridges. Class 2 moraines have distinct crestlines, typically occur in nested groups and range in height from ~1 to 20 m. Class 3 moraines are small (~1–10 m height), have distinct crestlines and are mostly composed of angular boulders with little vegetation cover. Class 3 moraines are only found at Lough Nahanagan, Kelly's Lough, North Prison, Lough Cleevaun and Lough Ouler (Fig. 5), restricted to high-elevation cirques (400–684 m a.s.l.). Where Class 3 moraines are found in the same valley as Class 1 and 2 moraines, they are always located upvalley of them.

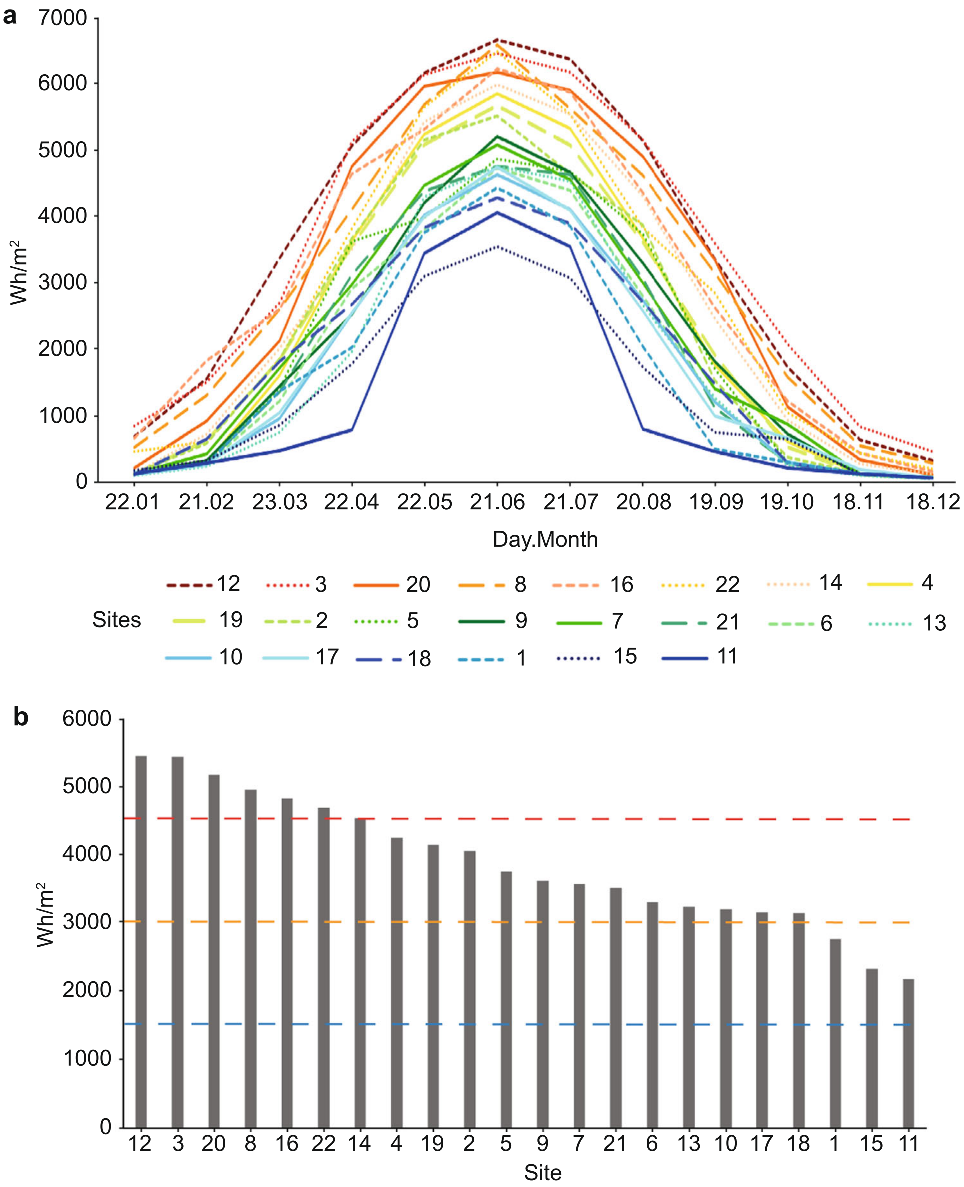

Figure 3. (a) Accumulated radiation over one calendar year for each of the 22 potential NS glacier-hosting sites. Sites are organised from high (red) to low (blue) radiation values. (b) Average radiation over the 6 days modelled from April to September at the 22 sites. The coloured dashed lines define high radiation (4500 Wh m^{-2}) in red, medium radiation (3000 Wh/m²) in orange and low radiation (1500 Wh m^{-2}) in blue. Numbered locations: (1) North Prison, (2) Asbawn, (3) South Prison, (4) Upper Fraughan Rock Glen, (5) Glenreeemore, (6) Lower Fraughan Rock Glen, (7) Kelly's Lough, (8) Glenmalure, (9) Firrib, (10) Lough Cleevaun, (11) Lough Nahanagan, (12) Upper Glenmacnass, (13) Glendalough, (14) Lugacullen, (15) Lough Ouler, (16) Lower Glenmacnass, (17) Lower Lough Bray, (18) Upper Lough Bray, (19) Lough Dan, (20) Lough Tay, (21) Raven's Glen and (22) Glensoulan. See Figs. 1 and 2 and Table S1 for more information on the numbered sites. [Color figure can be viewed at wileyonlinelibrary.com]

The difference in the composition of Class 3 moraines compared to classes 1 and 2 may relate to different glacier and glaciofluvial dynamics. The lack of finer-grained sediment and angularity of the boulders within Class 3 moraines could be a result of predominantly supraglacial or englacial debris transport pathways, whereby supraglacial material from rockfall was dumped at the ice margin (Shakesby, 1989; Winkler and Matthews, 2010; Barr and Spagnolo, 2015). Limited production of subglacially derived material may be the result of short transport distances, which fits with Class 3 moraines always being located close to valley heads. The absence of finer-grained material may have been caused by meltwater winnowing (e.g., Winkler, 2020; Boston et al., 2023). Lithology may also have played a role since most Class 3 moraines are composed of granite, which has a high resistance to erosion (Lukas et al., 2013; Matmon et al., 2020). At Lough Ouler (Fig. 5e), Class 3 moraines are composed of shale and schists and, although they are still boulder-dominant, there is a larger volume of intra-boulder sedimentary material (matrix).

We also attribute some of these observed differences in moraine morphology, particularly sharp versus subdued or rounded crestlines, to variations in climatic conditions during postdepositional stabilisation (Barr and Lovell, 2014). Following ice retreat, moraines often degrade, flattening and widening as fine-grained sediments are redistributed downslope away from the moraine crest (Hallet and Putkonen, 1994). Pre-LLS moraines in Britain, for example, were exposed to periglacial conditions and eroded during the LLS (Ballantyne, 2019). In contrast, moraines formed during the LLS would have stabilised relatively quickly due to vegetation regrowth as a result of rapid climate amelioration at the start of the Holocene (Lukas, 2006).

Other lines of evidence that have previously been used in Scotland to identify LLS glacier limits (e.g., Lukas, 2006, Boston et al., 2015) include boulder spreads, thick valley side sediment accumulations (drift limits) and well-developed talus

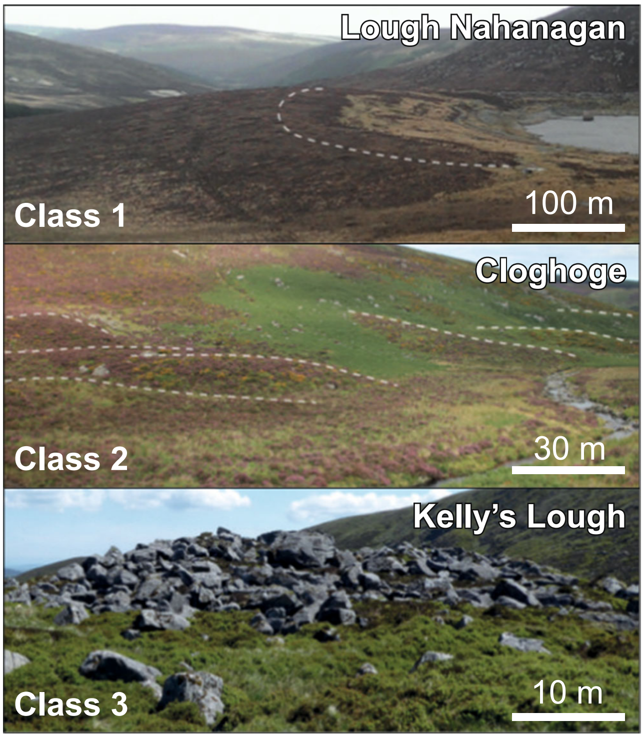

Figure 4. Examples of the three moraine classifications identified in the Wicklow Mountains (adapted from Knight et al., 2023). [Color figure can be viewed at wileyonlinelibrary.com]

slopes. Boulder spreads occur at all cirques where there are Class 3 moraines (Fig. 5), excluding the submerged Lough Nahanagan site (Fig. 5a). In the other cirques, the lower limit of boulder spreads coincides with the outermost Class 3 moraine. However, boulder spreads are also found to be associated with Class 2 moraines. Drift limits are notably absent from the Class 3 moraine cirque sites and occur either in association with Class 1 and Class 2 moraines, or most notably, beyond the downvalley limit of Class 3 moraines. Finally, mature (thick, well-developed) talus accumulations are absent near Class 3 moraines, with only thinner more immature talus slopes found at North Prison (Fig. 5c). However, mature talus is found at several cirques with Class 2 moraines (e.g., Lough Tay, South Prison, Lower Fraughan Rock Glen). River terraces have been relied on heavily as part of the morphostratigraphic signature at Scottish LLS glacier sites (e.g., Boston et al., 2015; Chandler et al., 2019), but are rare in the Wicklow Mountains and only become apparent much further downvalley beyond most moraines (Knight et al., 2023).

Using the geomorphology at Lough Nahanagan and Kelly's Lough (Fig. 5a, b), as the two established examples of NS glaciation in the Wicklow Mountains, alongside the expected morphostratigraphic relationships described above (Lukas, 2006), we suggest that NS glaciers in the Wicklow Mountains are associated with Class 3 moraines. Both established NS examples contain Class 3 moraines dated to the NS, and moraines beyond the established glacier limits are either Class 1 (Lough Nahanagan; dated to 22.4 ± 1.3 ka; recalculated ^{36}Cl age from Bowen et al., 2002) or absent (Kelly's Lough). It is important to note that Tomkins et al. (2018) calculated a NS age for the outer (Class 1) moraine at Lough Nahanagan (Fig. 5a) using the SHED technique. However, based on the morphostratigraphic principles described above, we suggest that the broad, subdued nature of this moraine indicates that it has been subjected to prolonged periglacial conditions and therefore relates to an earlier phase of glaciation more consistent with the Bowen et al. (2002) recalculated ^{36}Cl age of 22.4 ± 1.3 ka for this moraine. We therefore suggest that the other undated sites that contain Class 3 moraines (North Prison, Lough Cleevaun and Lough Ouler) (Fig. 5) are potential sites of NS cirque glaciation.

There are several other potential glacier-hosting sites that contain moraines (e.g., Upper and Lower Lough Bray, Lower Fraughan Rock Glen, Glen Firrib and Glen Asbawn), but these are predominantly Class 2 and some Class 1 moraines. Whilst Class 2 moraines have distinct crestlines and are therefore comparable to moraines elsewhere that have been dated to GS-1 (e.g., Finlayson et al., 2011; Gheorghiu et al., 2012), they are widespread in the Wicklow Mountains and are often located well beyond cirques (e.g., Glensoulan, Cloghoge, Leoh Valley) (Fig. 1) (Knight et al., 2023). They are also associated with mature talus at several locations and therefore do not fit a NS morphostratigraphic signature. We also note that in some areas of Scotland, similar moraines have been interpreted as being older than the LLS (e.g., Chandler et al., 2019). However, Tomkins et al. (2018) obtained NS SHED ages from Class 2 moraines at Upper Lough Bray (12.3 ± 0.5 ka) and Upper Glenmacnass (11.4 ± 0.1 ka). Taking this into consideration, we suggest that some, but certainly not all, Class 2 moraines may also be NS in age. The Class 2 moraines at Upper Lough Bray and Upper Glenmacnass contain a large number of very large boulders, similar to Class 3 moraines. The other possible NS glacier-hosting site to highlight is Upper Fraughan Rock Glen, which is a high-elevation north-facing cirque comparable to Lough Cleevaun. However, no moraines are found in this cirque, so we do not consider this site further.

Surface exposure ages

Three out of the four samples from boulders located on different Class 3 moraines at Kelly's Lough have exposure ages between 10.2 ± 0.8 and 12.2 ± 0.9 ka, yielding a mean landform age representative of coeval moraine formation of 11.1 ± 0.6 ka (Fig. 6a and Table 1), comparable to the ^{10}Be moraine age of 10.8 ± 0.5 ka from the same site (Barth et al., 2018). These ages comply with the morphostratigraphical position of the Class 3 moraines and together confirm a NS age for moraines at Kelly's Lough. A fourth sample (KL-2) is rejected, as it is clearly an outlier when compared to the mean of the remaining three accepted samples, which cluster within 1 sigma of the arithmetic mean.

The moraines at Upper and Lower Lough Bray consist of a large Class 1 moraine bounding Lower Lough Bray and a series of narrower Class 2 moraines at the edge of Upper Loch Bray and upvalley of the Class 1 moraine (Fig. 5f). The Class 1 moraine at Lower Lough Bray (LBO-3) has a mean exposure age of 21.3 ± 2.0 ka, which fits with the ^{10}Be exposure ages of ~21 ka from Ballantyne et al. (2006; recalculated by Tomkins et al., 2018) that track the deglaciation of the independent ice dome following its separation from the British–Irish Ice Sheet. Samples LBO-1 and LBO-2 obtained from boulders not on moraines but beyond the Lower Lough Bray Class 1 moraine (Fig. 5f) have similar ages (Table 1), possibly indicating retreat of ice from the Lower Lough Bray limit sometime between 21.3 and 24.4 ka.

All five samples from the crestline of the largest of the Class 2 moraines at Upper Lough Bray have relatively consistent mean ages ranging from 9.7 ± 1.6 to 12.1 ± 1.4 ka, yielding a mean moraine age of 11.2 ± 0.6 ka (Fig. 6b and Table 1) and supporting the assertion by Tomkins et al. (2018) that Upper Lough Bray hosted a NS glacier.

A mean exposure age of 19.7 ± 2.4 ka was also obtained from a Class 2 moraine at Lough Tay (Tables 1 and S2; see

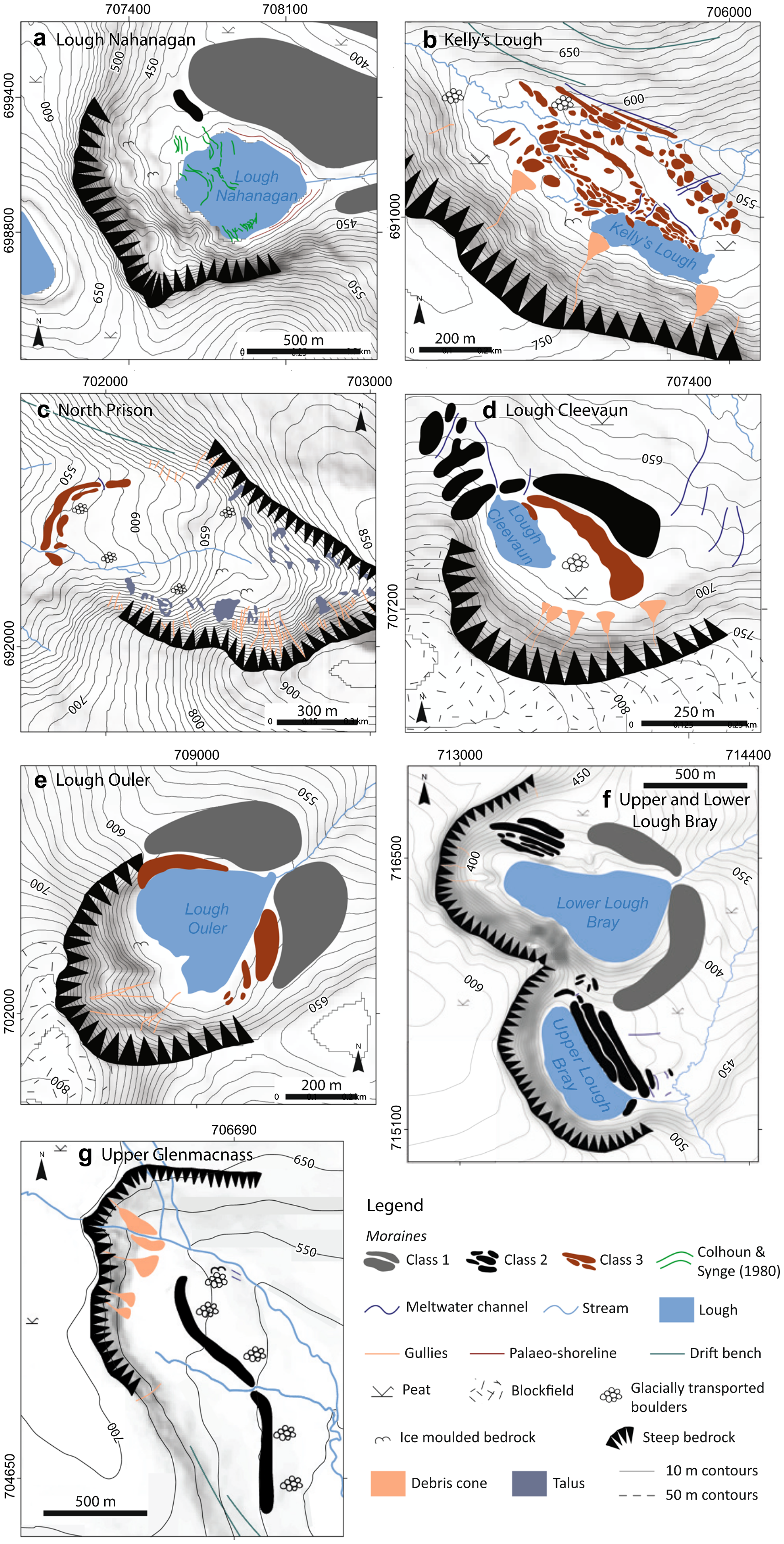

Figure 5. Geomorphological maps of the seven likely NS glacier-hosting sites. (a) Lough Nahanagan. (b) Kelly's Lough. (c) North Prison. (d) Lough Cleevaun. (e) Lough Ouler. (f) Upper and Lower Lough Bray (only Upper Lough Bray is considered a NS glacier-hosting site). (g) Upper Glenmacnass. Grid references are Irish Transverse Mercator (units: metres). [Color figure can be viewed at wileyonlinelibrary.com]

Fig. 1 for location), which indicates that this moraine was formed during or shortly after the LLGM.

Sites that hosted Nahanagan Stadial glaciers

We suggest that North Prison, Lough Cleevaun, Lough Ouler, Upper Lough Bray and Upper Glenmacnass hosted NS glaciers, in addition to the established sites of Lough Nahanagan and Kelly's Lough (Fig. 5). North Prison, Lough Cleevaun and Lough Ouler contain Class 3 moraines and fit our interpretation of the NS morphostratigraphic signature for the Wicklow Mountains. These sites also had lower annual solar radiation due to topographic shading, with most sites lying northeast of northwest–southeast trending ridges with high radiation values and leeward of the

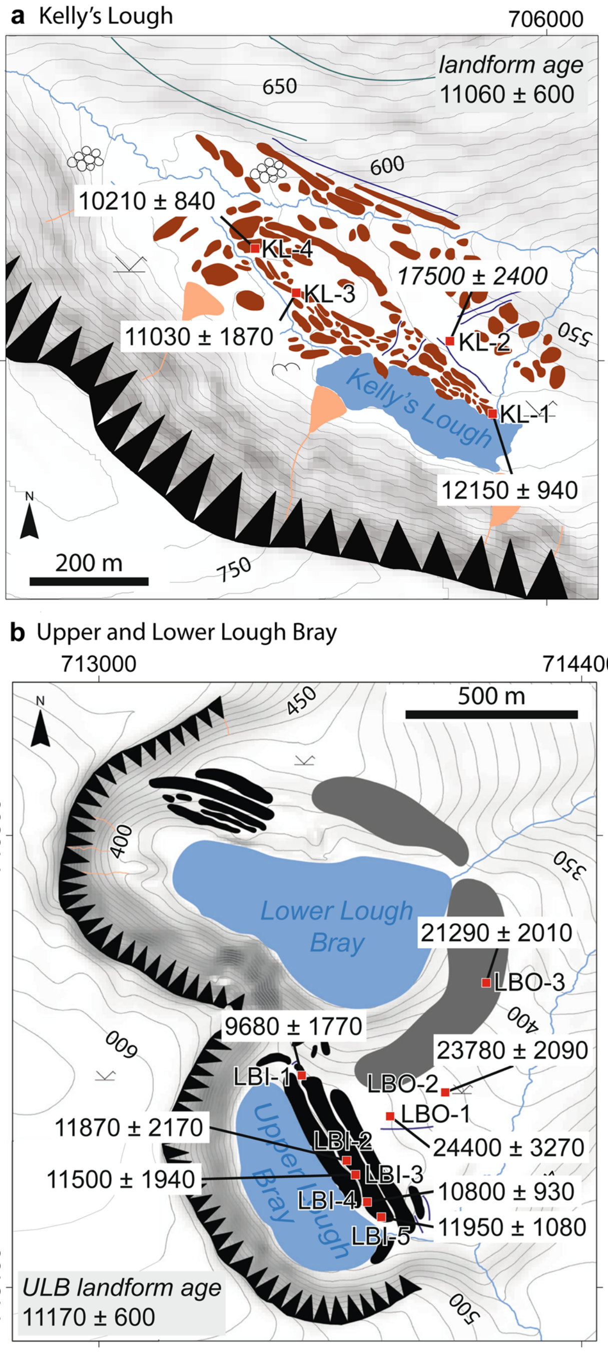

Figure 6. Surface exposure sample locations (red squares) and weighted mean exposure ages (a^{-1}; based on paired ^{26}Al and ^{10}Be ages where available) shown on the geomorphological maps of (a) Kelly's Lough; and (b) Upper and Lower Lough Bray. Landform ages are reported for Kelly's Lough and Upper Lough Bray (ULB); see Table 1 for further details on how these were calculated. The legend is the same as in Fig. 5. See Table 1 and Tables S2, S7 and S8 for more details on the ages. Grid references are Irish Transverse Mercator (units: metres). [Color figure can be viewed at wileyonlinelibrary.com]

dominant southwest wind direction (Figs. 2 and 3). Upper Lough Bray and Upper Glenmacnass, whilst containing Class 2 rather than Class 3 moraines, are NS in age based on our exposure ages and the Tomkins et al. (2018) SHED ages.

Glacier reconstruction, palaeo-ELAs and palaeoprecipitation

The seven reconstructed glaciers are small, with an average glacier area of 0.40 km^2 at their maximum extent (Fig. 7). Equilibrium line altitudes using an AABR of 1.56 range between 470 ± 5 and 721 ± 5 m a.s.l. (Table 2), with an average ELA of 599 m a.s.l.

The calculated palaeoprecipitation values for NS glaciers in the Wicklow Mountains are presented in Table 3 and range from 2081 ± 391 to 2713 ± 370 mm a^{-1} (at the ELA) and from 1387 ± 332 to 2084 ± 327 mm a^{-1} (at sea level). These precipitation estimates are reliant on the reliability of the July temperature proxy used and the method used to convert July temperature into the mean summer temperature. Use of a sinusoidal function here, rather than the equation suggested by Benn and Ballantyne (2005) that has been used in many British GS-1 glacier reconstructions, results in palaeoprecipitation estimates that are ~400 mm lower. This demonstrates the importance of the approach used to estimate palaeoprecipitation and highlights the limitations of comparing palaeoprecipitation estimates across regions if different methodologies have been used.

ELA lowering from windblown snow and avalanching

Potential snowblow areas and PAAs are shown in Fig. 8 as a distribution map, in Table 4 as a total for each glacier and in Fig. 9 broken down by wind direction sectors. Fig. 8 and Table 4 show that the Upper Lough Bray glacier had the highest potential for enhanced accumulation through snowblow due to a large plateau area to the south and west (snowblow factor: 8.37). Other glaciers with comparatively high snowblow factors are Upper Glenmacnass, Lough Cleevaun and Lough Nahanagan. In contrast, the glaciers at North Prison, Kelly's Lough and Lough Ouler had the lowest snowblow factors. These three glaciers, along with the Lough Cleevaun glacier, had similar avalanche factors (~0.46), whilst the glaciers at Upper Lough Bray, Upper Glenmacnass and Lough Nahanagan had the highest avalanche factors (0.51–0.64).

Discussion

Geomorphological signature of Nahanagan Stadial glaciation in the Wicklow Mountains

The Wicklow Mountains represent an example of marginal glaciation in Britain and Ireland during GS-1. We find that the restricted size of NS glaciers, often only partially occupying their cirques, overall resulted in fewer landforms (especially glaciofluvial) than those found at other sites glaciated during GS-1 (e.g., Northwest Highlands and Monadhliath Mountains, Scotland) (Lukas, 2006; Boston et al., 2015). This has an impact on the use of morphostratigraphy to identify NS glaciation in the absence of numerical ages (e.g., Lukas, 2006) because there are fewer lines of evidence that can be used to identify NS glacier limits.

In Scotland, the relationship between glaciofluvial terraces and moraines (concurrence of the outermost moraine with the initiation of a glaciofluvial terrace) can help identify LLS limits (e.g., Lukas, 2006; Finlayson, 2006; Boston et al., 2015; Chandler et al., 2019). We do not identify such a relationship in the Wicklow Mountains. This is likely because NS ice extent was restricted to small high-elevation cirque glaciers, and thus the likelihood of well-developed terraces beyond the NS limits is low because of the steeper topography and limited fine-grained sediment aggradation (Menting et al., 2015; Kirkbride and Deline, 2018).

Talus slope characteristics are also used as a line of evidence to identify GS-1 glacier limits; mature talus slopes only occur beyond GS-1 glacier margins due to their development under

Table 1. Surface exposure ages.

Sample	Lab code	[^{10}Be] (10^4 atoms g^{-1})	^{10}Be exposure age (a^{-1})†	[^{26}Al] (10^6 atoms g^{-1})	[^{27}Al] (ug g^{-1})	^{26}Al exposure age (a^{-1})†	Boulder exposure age (a^{-1})‡	Landform age (a^{-1})§
Kelly's Lough								
KL-1	OZ-918	9.00 ± 0.36	12 400 ± 500	5.56 ± 0.53	110	10 800 ± 1000	12 150 ± 940	
KL-2	OZ-919	13.55 ± 2.08	*19 000 ± 2900*	8.10 ± 1.45	515	*16 100 ± 2900*	*17 500 ± 2400*	11 060 ± 600
KL-3	OZ-920			5.64 ± 0.87	212	11 000 ± 1700	11 030 ± 1870	
KL-4	OZ-921	7.29 ± 0.34	9900 ± 500	7.29 ± 0.83	188	13 900 ± 1600	10 210 ± 840	
Lough Bray								
LBO-1	OZ-922			11.26 ± 1.27	245	24 400 ± 2800	24 400 ± 3270	
LBO-2	OZ-923	14.04 ± 0.95	22 000 ± 1500	12.78 ± 1.07	138	28 300 ± 2400	23 780 ± 2090	
LBO-3	OZ-924	13.09 ± 0.97	21 100 ± 1600	9.68 ± 1.15	194	22 000 ± 2600	21 290 ± 2010	
LBI-1	OZ-926			4.44 ± 0.74	282	9680 ± 1630	9680 ± 1770	
LBI-2	OZ-927			5.39 ± 0.90	190	11 900 ± 2000	11 870 ± 2170	
LBI-3	OZ-928	1.90 ± 0.17	*2900 ± 300*	5.17 ± 0.79	233	11 500 ± 1800	11 500 ± 1940	11 170 ± 600
LBI-4	OZ-929	6.78 ± 0.36	10 700 ± 600	5.42 ± 0.87	195	12 000 ± 1900	10 800 ± 930	
LBI-5	OZ-930	7.61 ± 0.50	11 900 ± 800	5.51 ± 0.62	162	12 100 ± 1400	11 950 ± 1080	
Lough Tay								
LT-5	OZ-1205	12.27 ± 1.80	22 800 ± 3400	6.89 ± 0.88	189	18 100 ± 2300	19 660 ± 2360	

See Fig. 6 and Table S2 for sample locations, and Tables S2, S7 and S8 for more details on the ages.
†Internal error.
‡Weighted mean of ^{10}Be and ^{26}Al ages. Final boulder age errors are given by the weighted mean error in quadrature with an estimated 7% local production rate uncertainty. Italicised ages are rejected as outliers.
§Landform age and error are calculated as the weighted mean of all accepted boulder ages for the given landform (LBI samples) or set of coeval landforms (KL samples) and as the weighted mean error, respectively.

intense periglacial conditions during GS-1 (e.g., Ballantyne and Eckford, 1984; Lukas, 2006; Ballantyne, 2007a). In the Wicklow Mountains, talus slopes are rare, probably because of the region's rolling topography with few high-level cliffs and rock faces. Therefore, talus development is limited to just a few sites with steeper terrain (e.g., mature talus at Glenmalure, Lower Fraughan Rock Glen, Glendalough, South Prison, Lough Tay and immature talus at North Prison). Comparatively, in Eryri, significant talus development is found both inside and outside of inferred LLS ice limits, but is not present in all cirques (Bendle and Glasser, 2012). At Ben More Coigach in Scotland, talus is also more extensive due to steeper alpine-style topography, but is entirely absent within the inferred LLS ice limits (Chandler and Lukas, 2017). Thus, talus slope characteristics could not be used widely in the Wicklow Mountains as a complementary line of evidence for identifying NS glacier limits, and we suggest that this is because of the overall more subdued upland topography.

Perhaps the largest implication of fewer lines of geomorphological evidence is that variations in moraine morphology (e.g., Fig. 4) have played an overly prominent role in defining NS glacier extents. Nonetheless, the existence of multiple absolute ages at two sites, Lough Nahanagan and Kelly's Lough, has enabled us to identify a NS glacial geomorphological signature with some confidence. This signature consists of restricted cirque glaciation characterised by narrow, sharp-crested partially openwork (Class 3) moraines within a zone heavily strewn with boulders.

We thus suggest that the presence of Class 3 moraines is a clear indicator of NS glaciation in the Wicklow Mountains (Figs. 4 and 5) (Knight et al., 2023). We argue that differences in moraine morphology (classes 1–3) in the Wicklow Mountains are related to debris source and transport pathways, processes of formation (Benn and Evans, 2010), postdepositional stabilisation (Hallet and Putkonen, 1994) and relatively short transport distances from cirque headwall to glacier terminus (maximum 1.1 km, average 550 m across all seven sites), which in part may be related to age (Lukas, 2006). The bouldery nature of Class 3 moraines is relatively unusual compared to most moraines associated with other GS-1 glaciated sites in Britain and Ireland (e.g., Barr et al., 2017b; Bickerdike et al., 2018), but does share similarities with LLS moraines in Scotland on Arran (Ballantyne, 2007a), North Harris (Ballantyne, 2007b) and in the Cairngorms (Standell, 2014). Bouldery Little Ice Age (Neoglacial) and GS-1 moraines are also reported in Norway (e.g., Rea and Evans, 2007; Winkler and Matthews, 2010; Ffoulkes and Harrison, 2014) and Sweden (Dahl et al., 1997). The NS Class 3 moraines at Lough Nahanagan vary somewhat from those at other sites in the Wicklow Mountains, likely due to their subaqueous formation within the lough. Here, there is evidence for moraine formation through both dump and push processes (Colhoun and Synge, 1980). The lough would have provided a favourable setting for ice-marginal pushing of proglacial material, as ice was advancing into soft deformable lake sediments (e.g., Boulton and Eyles, 1979; Bentley, 1996). It is possible that there are similar push moraines in other loughs in the Wicklow Mountains.

All ages from Class 3 moraines, both published previously (Barth et al., 2018; Tomkins et al., 2018) and presented here (Fig. 5b and Table 1), provide NS ages. The ages from Class 1 moraines are ~21–22 ka at Lough Nahanagan (Bowen et al., 2002) and Lower Lough Bray (Fig. 5f and Table 1), with the exception of a SHED age at Lough Nahanagan of 10.9 ka (Tomkins et al., 2018). In contrast, ages on Class 2 moraines are mixed. The mean exposure age is 19.7 ± 2.8 ka for a Class 2 moraine at Lough Tay (Fig. 1 and Table 1). Most SHED ages on Class 2 moraines are pre-NS (~15–16 ka), apart from those at Upper Lough Bray and Upper Glenmacnass (Tomkins et al., 2018). We also present NS exposure ages from a Class 2 moraine at Upper Lough Bray (Table 1), in agreement with Tomkins et al. (2018). An additional recalculated ^{36}Cl age of 14.3 ± 1 ka (Bowen et al., 2002) from this same moraine suggests that, on the balance of probability, NS glacier ice reached the Class 2 moraines at Upper Lough Bray and Upper Glenmacnass, as we have reconstructed in Fig. 7.

This range of ages on Class 2 moraines presents an interesting geomorphological problem. Class 2 moraines are

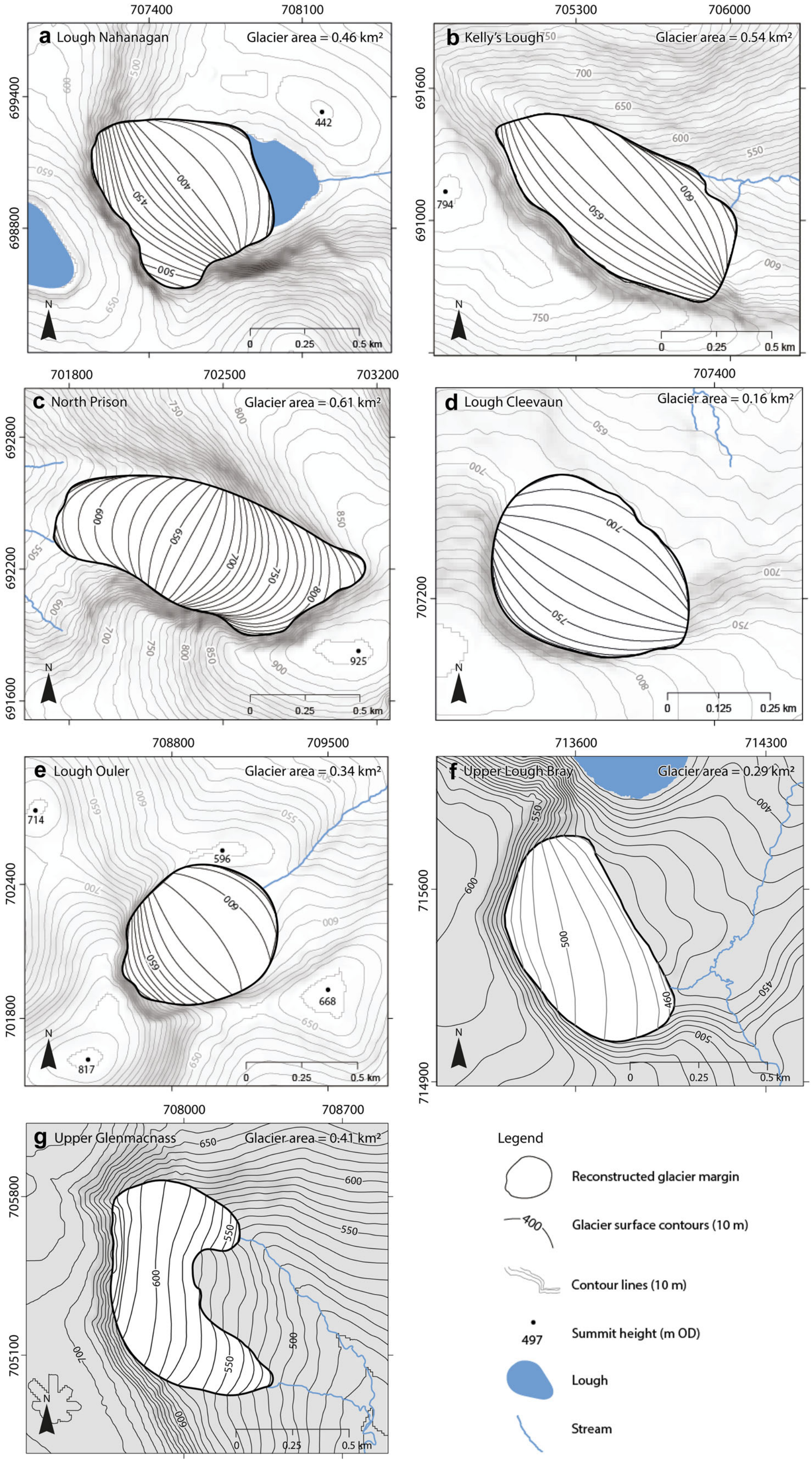

Figure 7. Glacier reconstructions of the seven Nahanagan Stadial glaciers. Grid references are Irish Transverse Mercator (units: metres). [Color figure can be viewed at wileyonlinelibrary.com]

the most numerous and spatially extensive moraines identified in the Wicklow Mountains and are found both in cirques (e.g., Upper and Lower Lough Bray, Lough Cleevaun, Lower Fraughan Rock Glen, Glenreemore), including close to the headwall (e.g., Upper Lough Bray, Upper Glenmacnass), and in valleys leading from plateau areas (e.g., Lower Glenmacnass, Cloghoge, Glensoulan, Stonecutter's Glen) (Knight et al., 2023). As noted above, the two Class 2 moraines with NS ages in Tomkins et al. (2018) and this study are situated close to their cirque backwalls (<500 m) and are also heavily covered in large angular boulders. In this respect, they are similar to Class 3 moraines, but are significantly larger and are generally less openwork. At Upper Lough Bray, the dated Class 2 moraine is particularly large (7 m in height with a base width

Table 2. Equilibrium line altitudes (ELAs) for Nahanagan Stadial glaciers in the Wicklow Mountains.

Glacier (site number)	Area (km^2)	AAR 0.5 (m a.s.l.)	AAR 0.6 (m a.s.l.)	AABR 1.56 (m a.s.l.)	AABR 1.67 (m a.s.l.)	AABR 1.8 (m a.s.l.)	AABR 1.9 ± 0.81 (m a.s.l.)	AABR 2.0 (m a.s.l.)
Lough Nahanagan (11)	0.46	465	453	**470**	469	468	467 ± 9	467
Kelly's Lough (7)	0.54	632	627	**633**	633	632	631 ± 6	631
North Prison (1)	0.61	675	655	**679**	677	675	673 ± 18	671
Lough Cleevaun (10)	0.16	718	712	**721**	720	719	719 ± 5	718
Lough Ouler (15)	0.34	608	604	**617**	616	615	615 ± 5	614
Upper Lough Bray (18)	0.29	487	482	**489**	488	488	487 ± 5	487
Upper Glenmacnass (12)	0.41	585	577	**582**	581	580	579 ± 7	579

Following Pellitero et al. (2015), the maximum error on all ELAs, unless otherwise specified, is ±5 m, which is half of the 10 m contour interval used. In the text, we report the ELAs calculated using an AABR of 1.56 (shown in bold here).

Table 3. Palaeoprecipitation values for each reconstructed Nahanagan Stadial glacier calculated using the temperature–precipitation relationship defined by Ohmura et al. (1992).

Glacier	ELA (AABR 1.56) (m a.s.l.)	Effective precipitation at ELA (mm a^{-1})	Effective precipitation at sea level (mm a^{-1})
Lough Nahanagan	470 ± 5	2713 ± 370	2084 ± 327
Kelly's Lough	633 ± 5	2297 ± 379	1609 ± 330
North Prison	679 ± 5	2183 ± 385	1491 ± 331
Lough Cleevaun	721 ± 5	2081 ± 391	1387 ± 332
Lough Ouler	617 ± 5	2337 ± 377	1652 ± 330
Upper Lough Bray	489 ± 5	2664 ± 357	2024 ± 326
Upper Glenmacnass	582 ± 5	2425 ± 372	1749 ± 329

of 30–35 m) and is the centremost of two similar, but lower ridges (Fig. 5f). We suggest that this moraine was formed during several glacial advances, forming a composite feature that has resulted in a more ambiguous NS glacial geomorphological signature here. Together, this suggests that the characteristics of Class 2 moraines do not align with a single glacial event.

Glaciation style

All seven NS glaciers were small and only partially filled the cirques that they occupied. The glaciers formed beneath north-facing to east-facing slopes in highly shaded areas and in the lee of the prevailing south-west wind for higher snow accumulation, as is common in the northern hemisphere (e.g., Evans, 1977; Barr et al., 2017a). At Kelly's Lough and Upper Glenmacnass, the NS glaciers have not developed at the valley heads (which have an ~southeast aspect), but rather beneath the ~northeast-facing side valley slopes (Fig. 7). The glacier shape at these locations was therefore more elongate than circular, and ice flow would have been predominantly north or eastwards, away from the most shaded valley side wall (i.e., the NS glacier's backwall), rather than directly following the main valley orientation. Similar glacier configurations are recognised in Bannau Brycheiniog, Wales (Carr and Coleman, 2007; Coleman and Carr, 2008), and the Galloway Hills, Scotland (Cornish, 1981). The North Prison NS glacier was likely similarly influenced by shading from its north-facing side wall, although here, the moraine distribution and valley slope indicate that the glacier did predominantly flow westwards following the main valley orientation (Fig. 7c), making this glacier somewhat of an anomaly that is worth further investigation.

Upper Lough Bray is an interesting case because the NS glacier was probably hemmed in by a large pre-existing moraine. Similar to the other cirque locations, ice flow would have been predominantly north-eastwards away from the cirque backwall, but smaller moraines at the northern and southeastern edges of the cirque indicate ice flow in both northern and southeastern directions, escaping the constraints of the large frontal moraine. We reconstruct a similar configuration and ice flow pattern for the Upper Glenmacnass NS glacier (Fig. 7g) based on meltwater channels and scattered boulders at either end of the main moraine (Fig. 5g).

There is a clear north-easterly aspect for six of the seven NS cirques identified here, with the west-facing North Prison being the exception. This demonstrates the importance of topographic shading and the potential for enhanced snow accumulation in the lee of the prevailing wind direction (from the southwest) in areas of marginal glaciation. There are also considerations for long-term cirque and landscape development here. Enlarged cirques or valley heads may be partially occupied during periods of time where the climate is close to the glaciation threshold. This may result in uneven erosion of the cirque back or side walls, leading to compound cirques (e.g., Barr and Spagnolo, 2015). An interesting question also arises as to whether a similar pattern of glaciation occurs in reverse as an area deglaciates, or whether due to hysteresis, existing glacier ice in the full cirque changes the pattern of deglaciation compared to glacier growth.

Importance of windblown snow in marginal glaciation settings

The snowblow analysis indicates that several of the NS glaciers likely benefitted from enhanced snow accumulation via wind-blown snow and avalanching (i.e., local rather than regional climatic factors). This is particularly significant for Lough Nahanagan, as it is the Irish NS/GS-1 type site (Colhoun and Synge, 1980), and yet, this glacier's ELA is probably not truly representative of regional climatic conditions at the time. The glacier's ELA (470 ± 5 m a.s.l.) is lower than all other calculated NS ELAs (489–721 m a.s.l.). The glacier has a PSBA of 2.46 km^2 (third largest) and associated snowblow factor of 2.31.

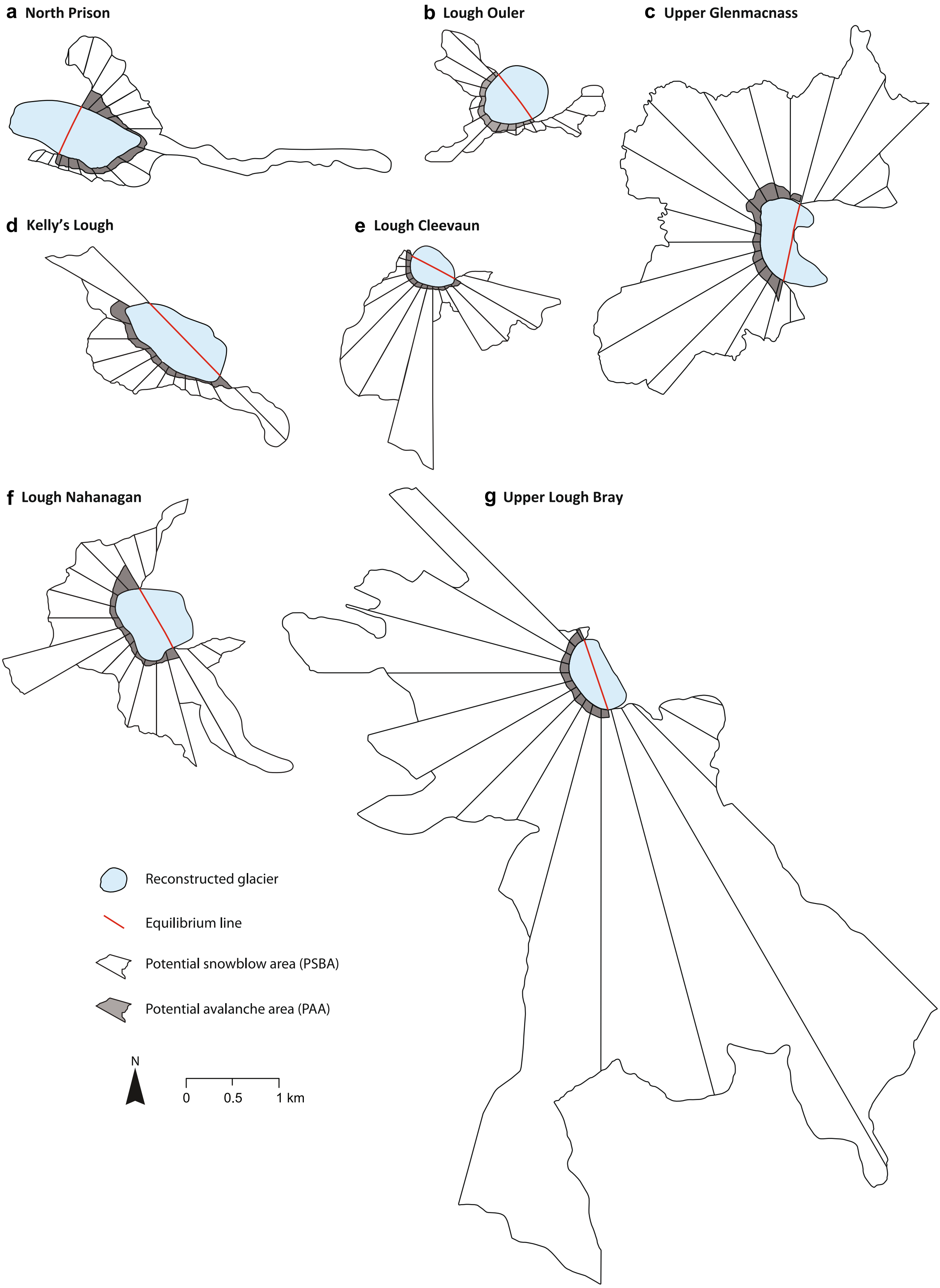

Figure 8. Distribution of potential snowblow and avalanche areas around the reconstructed Nahanagan Stadial glaciers, produced using the approach of Mitchell (1996). Percentage values can be found in Table 4. Snowblow and avalanche areas broken down into 90° sectors for each glacier can be found in Fig. 9 and Tables S5 and S6. [Color figure can be viewed at wileyonlinelibrary.com]

The site also benefits from strong topographic shading and received the lowest amount of solar radiation throughout the ablation season (Fig. 3b). Comparatively, Lough Ouler received similarly low solar radiation levels but received less windblown snow and avalanching (Table 4), and is a smaller glacier with a higher ELA (0.34 km^2, ELA 617 ± 5 m a.s.l.).

Our reconstructed NS glacier at Upper Lough Bray also has a similarly low ELA (489 ± 5 m) to Lough Nahanagan and has a

Table 4. Calculated potential snowblow and avalanche areas based on Fig. 8 and approaches outlined by Sissons (1980) and Mitchell (1996).

Glacier (aspect)	Glacier area (km^2)	Total snowblow area (km^2)	Total snowblow ratio	Total snowblow factor	Total avalanche area (km^2)	Total avalanche ratio	Total avalanche factor
Lough Nahanagan (E)	0.46	2.46	5.35	2.31	0.12	0.26	0.51
Kelly's Lough (N)	0.54	1.02	1.89	1.38	0.11	0.21	0.46
North Prison (W)	0.61	1.55	2.54	1.59	0.13	0.21	0.46
Lough Cleevaun (N)	0.16	1.94	12.11	3.48	0.03	0.22	0.46
Lough Ouler (E)	0.34	0.58	1.71	1.31	0.07	0.20	0.45
Upper Lough Bray (E)	0.29	20.30	70.01	8.37	0.10	0.35	0.59
Upper Glenmacnass (E)	0.41	6.38	15.57	3.95	0.17	0.41	0.64

Snowblow and avalanche areas broken down into 90° sectors for each glacier can be found in Fig. 9 and Tables S5 and S6.

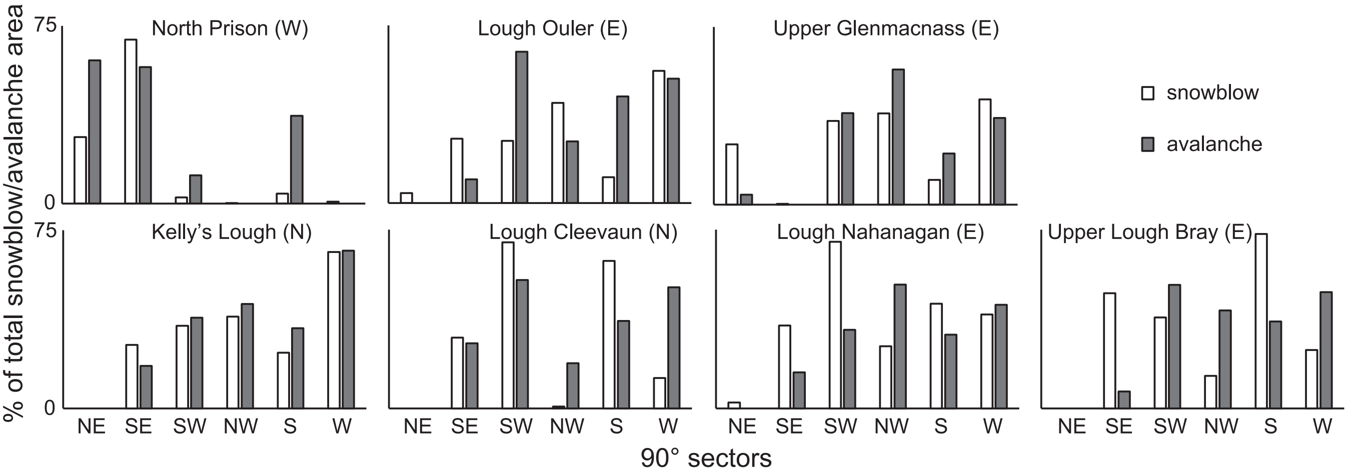

Figure 9. Snowblow and avalanche areas for each 90° sector as a percentage of the total snowblow/avalanche area. See Tables S5 and S6 for full data.

very large PSBA (20.3 km^2) and snowblow factor (8.37) due to being situated on the northeast edge of a plateau area. This glacier also received one of the lowest solar radiation totals during the ablation season (Fig. 3b), again suggesting that enhanced accumulation from windblown and avalanched snow, and high topographic shading, contributed to this glacier's low ELA. We therefore argue that the palaeoprecipitation values calculated in Table 3 are overinflated for Lough Nahanagan, Upper Lough Bray and Upper Glenmacnass (which also has a high PSBA and snowblow factor) due to windblown snow, and are therefore not representative of regional precipitation during the NS.

In contrast, Kelly's Lough, Lough Ouler and North Prison have the lowest snowblow factors and we therefore suggest that the ELAs calculated for these glaciers are more representative of a regional climatic ELA. On this basis, an average of these three ELAs provides a regional climatic ELA of 643 m, which is just over 40 m higher than the average ELA from all seven sites. Alternatively, since Kelly's Lough is the only site of these three with NS ages, arguably, its ELA of 633 ± 5 m best represents a regional climatic ELA.

Comparison with neighbouring regions of GS-1 marginal glaciation

Our reconstruction of NS ice extent in the Wicklow Mountains adds to a growing body of work documenting marginal glaciation in Britain and Ireland during GS-1. The topographic and latitudinal setting of the Wicklow Mountains is broadly comparable to the Mourne Mountains (Northern Ireland, 100 km to the northeast) and Eryri (Wales, 150 km to the east), both of which supported small cirque glaciers during GS-1 (Bendle and Glasser, 2012; Barr et al., 2017a). However, NS cirque glaciation in the Wicklow Mountains (seven glaciers, total area 2.81 km^2) is less extensive than both of these regions. Twenty-four NS glaciers (total area 5.24 km^2) have been identified in the Mourne Mountains and 38 LLS glaciers (total area 20.74 km^2) have been identified in Eryi. In contrast, in Macgillycuddy's Reeks (southwestern Ireland, 250 km to the southwest), just six small NS glaciers (total area 1.42 km^2) have been identified (Anderson et al., 1998), suggesting similarly restricted NS glaciation.

For the Wicklow Mountains, we have followed a conservative approach and have reconstructed two NS glaciers with high confidence (Lough Nahanagan, Kelly's Lough) and the remaining five with lower confidence. If some Class 2 moraines are associated with NS glaciation, five further cirques that contain small Class 2 moraines (Lower Fraughan Rock Glen, Glen Firrib, Glenreemore and Glen Asbawn) could be considered, alongside Upper Fraughan Rock Glen, which is high-elevation and has a north-facing aspect but does not contain any moraines. However, this evidence alone is not convincing enough for us to reconstruct NS glaciers at these locations. In comparison, in the absence of absolute ages, Barr et al. (2017b) reconstructed NS glaciers in all cirques in the Mourne Mountains based on SHED dating, but without considering differences in the morphostratigraphical context. Bendle and Glasser (2012) also reconstructed LLS glaciers in all cirques in Snowdonia, but arrived at this conclusion using a morphostratigraphic approach. Conversely, in Macgillycuddy's Reeks, absolute ages on moraines (Harrison et al., 2010;

Barth et al., 2018) demonstrate that not all cirques contained NS glaciers.

These methodological differences, particularly with the approach taken in the Mourne Mountains, make it difficult to directly compare ELAs across sites. However, with this point in mind, we can broadly compare reconstructed glaciers in these regions. NS glacier ELAs in the Wicklow Mountains (average ELA = 599 m a.s.l., regional climatic ELA = 633 ± 5 m a.s.l.) are at broadly comparable elevations to those in Macgillycuddy's Reeks (average ELA 689 m; Anderson et al., 1998) and Eryri (average 571 m a.s.l.; Bendle and Glasser, 2012), placing in the middle on a west to east transect of lowering ELAs. In contrast, ELAs in the Mourne Mountains have been calculated as much lower (average 475 ± 36 m a.s.l.; Barr et al., 2017a), which could, at least in part, be explained by the Mourne Mountains being situated further north, although we suspect that the methodological differences outlined above are also likely to have contributed to this. The average ELA in the Wicklow Mountains fits well with the latitudinal trend in regional GS-1 ELAs in western Britain spanning 53–57° N presented by Ballantyne (2007a), with higher average ELAs at lower latitudes.

For both the Mourne Mountains and Eryri, which have larger numbers of reconstructed GS-1 glaciers, distinct ELA gradients were identified (Bendle and Glasser, 2012; Barr et al., 2017a), with ELAs rising from west to east and southwest to northeast, respectively. We do not recognise any ELA gradients within the Wicklow Mountains, largely because the reconstructed glaciers are broadly positioned on a north–south transect (Fig. 1). The local-scale ELA gradients in the Mourne Mountains and Eryri may have been influenced by local topographic factors (Bendle and Glasser, 2012; Barr et al., 2017a). We also demonstrate that topography was likely a determining factor in glacier growth at several NS sites in the Wicklow Mountains, affecting shading, snowblow and avalanching. These observations have implications for palaeoclimatic reconstructions using small ice masses and could indicate that observed spatial variability, in both overall glacier extent and behavioural differences between local ice masses, may be more strongly connected to topographic differences than to a regional climate signal (Abermann et al., 2011). Snowblow and avalanche modelling must therefore be incorporated into any assessment of palaeoclimatic conditions based on cirque glaciers in order to investigate the reliability of palaeoprecipitation estimates.

Conclusions

We present evidence for seven cirque glaciers in the Wicklow Mountains, eastern Ireland, during the Nahanagan Stadial, which is the regional expression of Greenland Stadial-1 and equivalent to the Loch Lomond Stadial in Britain. Small cirque glaciers existed at Lough Nahanagan, Kelly's Lough, North Prison, Lough Cleevaun, Lough Ouler, Upper Lough Bray and Upper Glenmacnass. The sites were identified based on a combination of solar radiation modelling, glacial geomorphology and ^{10}Be and ^{26}Al surface exposure ages. The surface exposure ages from boulders on moraines at Kelly's Lough (10.2 ± 0.8–12.2 ± 0.9 ka) and Upper Lough Bray (9.7 ± 1.8–12.0 ± 1.1 ka) provide additional NS ages to those presented for Lough Nahanagan, Kelly's Lough and Upper Glenmacnass in previous work. Three-dimensional glacier reconstructions for the seven sites reveal small glaciers (average glacier area = 0.40 km^2) that only partially filled cirques. Equilibrium line altitudes range from 470 ± 5 m a.s.l. (Lough Nahanagan) to 721 ± 5 m a.s.l. (Lough Cleevaun), with an average ELA of 599 m a.s.l. Snowblow and avalanching contributions to glacier accumulation were significant for lowering some ELAs, demonstrating that local topography had an important role to play in sustaining marginal glaciers in the Wicklow Mountains during the NS.

Acknowledgements. We thank the following persons for their assistance during field campaigns: Josh Chambers, Fran Falcini, Arminel Lovell, Richard Delf, Lewys Atwell-Thomas, Dave Hardcastle and Pete Coxon. The Wicklow Mountains National Park granted permission to undertake the fieldwork. We thank Graeme Stewart, Stephan Tietz and Edmund Lovell for double-checking our maths. We are grateful to two anonymous reviewers for their detailed suggestions for improving the manuscript. This research was undertaken whilst Lauren Knight was funded by a University of Portsmouth PhD Bursary. Lauren Knight's fieldwork was funded by the Quaternary Research Association, the British Society for Geomorphology, the Royal Geographical Society and the International Association of Sedimentologists. Eric A. Colhoun and David Fink's fieldwork, sample preparation and AMS measurement for cosmogenic surface exposure ages were funded by an Australian Research Council Grant (Cosmogenic Isotope Dating of Glacial Deposits, 2002, Large ARC Grant A00000967).

Data availability statement

The data that support the findings of this study are available from the corresponding author upon reasonable request.

Conflict of interest statement—The authors declare no conflicts of interest.

Supporting information

Additional supporting information can be found in the online version of this article.

Table S1. Details of the 22 possible Nahanagan Stadial glacier-hosting sites, numbered from westernmost to easternmost. Cirque classifications are based on the Evans and Cox (1995) criteria. See Fig. 1 for locations.

Table S2. Sample details for surface exposure ages.

Table S3. Recalculated ^{36}Cl exposure ages from Bowen *et al.* (2002).

Table S4. Site data for recalculated ^{36}Cl exposure ages from Bowen et al. (2002).

Table S5. Potential snowblow areas (expressed as a percentage of total snowblow area) and snowblow factors for each 90° sector, calculated based on approaches outlined by Sissons (1980) and Mitchell (1996).

Table S6. Potential avalanche areas (expressed as a percentage of total avalanche area) and avalanche factors for each 90° sector, calculated based on approaches outlined by Sissons (1980) and Mitchell (1996).

Table S7. CRONUS V3 Uni Washington input file Wicklow data.

Table S8. CRONUS V3 Uni Washington output file Wicklow data.

References

Abermann, J., Kuhn, M. & Fischer, A. (2011) Climatic controls of glacier distribution and glacier changes in Austria. *Annals of Glaciology*, 52(59): 83–90.

Anderson, E., Harrison, S., Passmore, D.G., & Mighall, T.M. (1998) Geomorphic evidence of Younger Dryas glaciation in the Macgillycuddy's Reeks, south west Ireland. *Journal of Quaternary Science*, 13(6): 75–90.

Ballantyne, C.K. (2002) The Loch Lomond Readvance on the Isle of Mull, Scotland: glacier reconstruction and palaeoclimatic implications. *Journal of Quaternary Science*, 17(8): 759–771.

Ballantyne, C.K. (2007a) The Loch Lomond Readvance on north Arran, Scotland: glacier reconstruction and palaeoclimatic implications. *Journal of Quaternary Science: Published for the Quaternary Research Association*, 22(4): 343–359.

Ballantyne, C.K. (2007b) Loch Lomond Stadial glaciers in North Harris, Outer Hebrides, north-west Scotland: glacier reconstruction and palaeoclimatic implications. *Quaternary Science Reviews*, 26(25–28): 3134–3149.

Ballantyne, C.K. (2019) *Scotland's Mountain Landscapes: A Geomorphological Perspective*. Dunedin Academic Press Ltd.: Edinburgh & London.

Ballantyne, C.K., & Eckford, J.D. (1984) Characteristics and evolution of two relict talus slopes in Scotland. *Scottish Geographical Magazine*, 100(1): 20–33.

Ballantyne, C.K., McCarroll, D., & Stone, J.O. (2006) Vertical dimensions and age of the Wicklow Mountains ice dome, Eastern Ireland, and implications for the extent of the last Irish ice sheet. *Quaternary Science Reviews*, 25(17–18): 2048–2058.

Barr, I.D., Ely, J.C., Spagnolo, M., Clark, C.D., Evans, I.S., Pellicer, X.M. et al. (2017a) Climate patterns during former periods of mountain glaciation in Britain and Ireland: Inferences from the cirque record. *Palaeogeography, Palaeoclimatology, Palaeoecology*, 485: 466–475.

Barr, I.D., & Lovell, H. (2014) A review of topographic controls on moraine distribution. *Geomorphology*, 226: 44–64.

Barr, I.D., & Spagnolo, M. (2015) Glacial cirques as palaeoenvironmental indicators: Their potential and limitations. *Earth-Science Reviews*, 151: 48–78.

Barr, I.D., Roberson, S., Flood, R., & Dortch, J. (2017b) Younger Dryas glaciers and climate in the Mourne Mountains, Northern Ireland. *Journal of Quaternary Science*, 32(1): 104–115.

Barth, A.M., Clark, P.U., Clark, J., Roe, G.H., Marcott, S.A., McCabe, A.M. et al. (2018) Persistent millennial-scale glacier fluctuations in Ireland between 24 ka and 10 ka. *Geology*, 46(2): 151–154.

Bendle, J.M., & Glasser, N.F. (2012) Palaeoclimatic reconstruction from Lateglacial (Younger Dryas Chronozone) cirque glaciers in Snowdonia, North Wales. *Proceedings of the Geologists' Association*, 123(1): 130–145.

Benn, D.I., & Ballantyne, C.K. (2005) Palaeoclimatic reconstruction from Loch Lomond readvance glaciers in the west Drumochter Hills, Scotland. *Journal of Quaternary Science*, 20(6): 577–592.

Benn, D.I., & Evans, D.J.A. (2010) *Glaciers and Glaciation*. Routledge: London.

Benn, D.I., & Hulton, N.R. (2010) An ExcelTM spreadsheet program for reconstructing the surface profile of former mountain glaciers and ice caps. *Computers & Geosciences*, 36(5): 605–610.

Bentley, M. (1996) The role of lakes in moraine formation, Chilean Lake District. *Earth Surface Processes and Landforms*, 21(6): 493–507.

Bickerdike, H.L, Evans, D.J.A., Stokes, C.R., & Ó Cofaigh, C. (2018) The glacial geomorphology of the Loch Lomond (Younger Dryas) Stadial in Britain: a review. *Journal of Quaternary Science*, 33(1): 1–54.

Borchers, B., Marrero, S., Balco, G., Caffee, M., Goehring, B., Lifton, N. et al. (2016) Geological calibration of spallation production rates in the CRONUS-Earth project. *Quaternary Geochronology*, 31: 188–198.

Boston, C.M., Chandler, B.M.P., Lovell, H., Weber, P., & Davies, B.J. (2023) The role of topography in landform development at an active temperate glacier in Arctic Norway. *Earth Surface Processes and Landforms*, 48: 1783–1803.

Boston, C.M., Lukas, S., & Carr, S.J. (2015) A Younger Dryas plateau icefield in the Monadhliath, Scotland, and implications for regional palaeoclimate. *Quaternary Science Reviews*, 108: 139–162.

Boulton, G.S., & Eyles, N. (1979) Sedimentation by valley glaciers: a model and genetic classification. In *Moraines and Varves—Origin, Genesis, Classification, 11–23*, Schlüchter, M.C. (ed). A. A. Balkema: Rotterdam; 11–23.

Bowen, D.Q., Phillips F.M., McCabe, A.M., Knutz, P.C., & Sykes, G.A. (2002) New data for the last glacial maximum in Great Britain and Ireland. *Quaternary Science Reviews*, 21(1–3): 89–101.

Carr, S., & Coleman, C. (2007) An improved technique for the reconstruction of former glacier mass-balance and dynamics. *Geomorphology*, 92(1–2): 76–90.

Chandler, B.M.P., & Lukas, S. (2017) Reconstruction of Loch Lomond Stadial (Younger Dryas) glaciers on Ben More Coigach, north-west Scotland, and implications for reconstructing palaeoclimate using small ice masses. *Journal of Quaternary Science*, 32(4): 475–492.

Chandler, B.M.P., Boston, C.M., & Lukas, S. (2019) A spatially-restricted Younger Dryas plateau icefield in the Gaick, Scotland: Reconstruction and palaeoclimatic implications. *Quaternary Science Reviews*, 211: 107–135.

Chandler, B.M.P., Lovell, H., Boston, C.M., Lukas, S., Barr, I.D., Benediktsson, Í.Ö. et al. (2018) Glacial geomorphological mapping: a review of approaches and frameworks for best practice. *Earth-Science Reviews*, 185: 806–846.

Clark, C.D., Ely, J.C., Hindmarsh, R.C.A., Bradley, S., Ignéczi, A., Fabel, D., et al. (2022) Growth and retreat of the last British–Irish Ice Sheet, 31 000 to 15 000 years ago: the BRITICE-CHRONO reconstruction. *Boreas*, 51(4): 699–758.

Clerc, S., Buoncristiani, J.F., Guiraud, M., Desaubliaux, G., & Portier, E. (2012) Depositional model in subglacial cavities, Killiney Bay, Ireland. Interactions between sedimentation, deformation and glacial dynamics. *Quaternary Science Reviews*, 33: 142–164.

Coleman, C.G., & Carr, S.J. (2008) Complex relationships between Younger Dryas glacial, periglacial and paraglacial landforms, Brecon Beacons, South Wales. *Proceedings of the Geologists' Association*, 119(3–4): 259–276.

Coleman, C.G., Carr, S.J., & Parker, A.G. (2009) Modelling topoclimatic controls on palaeoglaciers: implications for inferring palaeoclimate from geomorphic evidence. *Quaternary Science Reviews*, 28(3–4): 249–259.

Colhoun, E.A., & Synge, F.M. (1980) The cirque moraines at Lough Nahanagan, County Wicklow, Ireland. *Proceedings of the Royal Irish Academy*, 80B: 25–45.

Coope, G.R., Lemdahl, G., Lowe, J.J., & Walkling, A. (1998) Temperature gradients in northern Europe during the last glacial–Holocene transition (14–9 ^{14}C kyr BP) interpreted from coleopteran assemblages. *Journal of Quaternary Science*, 13(5): 419–433.

Cornish, R. (1981) Glaciers of the Loch Lomond Stadial in the western Southern Uplands of Scotland. *Proceedings of the Geologists' Association*, 92(2): 105–114.

Coxon, P., Mitchell, F.J.G., & Wyse Jackson, P. (2012) *Wicklow in the Grip of an Ice Age*. Irish Quaternary Association: Dublin.

Dahl, S.O., Nesje, A., & Øvstedal, J. (1997) Cirque glaciers as morphological evidence for a thin Younger Dryas ice sheet in east-central southern Norway. *Boreas*, 26(3): 161–180.

DeBeer, C.M., Sharp, M.J. (2009) Topographic influences on recent changes of very small glaciers in the Monashee Mountains, British Columbia, Canada. *Journal of Glaciology*, 55(192): 691–700.

Evans, I.S. (1977) World-wide variations in the direction and concentration of cirque and glacier aspects. *Geografiska Annaler: Series A, Physical Geography*, 59(3–4): 151–175.

Ffoulkes, C., & Harrison, S. (2014) Evaluating the Schmidt hammer as a method for distinguishing the relative age of late Holocene moraines: Svellnosbreen, Jotunheimen, Norway. *Geografiska Annaler: Series A, Physical Geography*, 96(3): 393–402.

Fink, D., & Smith, A. (2007) An inter-comparison of ^{10}Be and ^{26}Al AMS reference standards and the ^{10}Be half-life. *Nuclear Instruments and Methods in Physics Research Section B: Beam Interactions with Materials and Atoms*, 259(1): 600–609.

Fink, D., Hotchkis, M., Hua, Q., Jacobsen, G., Smith, A.M., Zoppi, U. et al. (2004) The ANTARES AMS facility at ANSTO. *Nuclear Instruments and Methods in Physics Research Section B: Beam Interactions with Materials and Atoms*, 223–224: 109–115.

Finlayson, A.G. (2006) Glacial geomorphology of the Creag Meagaidh Massif, Western Grampian Highlands: implications for local glaciation and palaeoclimate during the Loch Lomond Stadial. *Scottish Geographical Journal*, 122(4): 293–307.

Finlayson, A., Golledge, N., Bradwell, T., & Fabel, D. (2011) Evolution of a Lateglacial mountain icecap in northern Scotland. *Boreas*, 40(3): 536–554.

Gheorghiu, D.M., Fabel, D., Hansom, J.D., & Xu, S. (2012) Lateglacial surface exposure dating in the Monadhliath Mountains, Central Highlands, Scotland. *Quaternary Science Reviews*, 41: 132–146.

Hallet, B., & Putkonen, J. (1994) Surface dating of dynamic landforms: young boulders on aging moraines. *Science*, 265(5174): 937–940.

Harrison, S., Glasser, N., Anderson, E., Ivy-Ochs, S., & Kubik, P.W. (2010) Late Pleistocene mountain glacier response to North Atlantic climate change in southwest Ireland. *Quaternary Science Reviews*, 29(27–28): 3948–3955.

Hofmann, F.M., Steiner, M., Hergarten, S., Preusser, F., & ASTER Team. (2024) Limitations of precipitation reconstructions using equilibrium-line altitudes exemplified for former glaciers in the Southern Black Forest, Central Europe. *Quaternary Research*, 117: 135–159.

Hughes, P.D. (2010) Little Ice Age glaciers in the Balkans: low altitude glaciation enabled by cooler temperatures and local topoclimatic controls. *Earth Surface Processes and Landforms*, 35(2): 229–241.

Humlum, O. (2002) Modelling late 20th-century precipitation in Nordenskiold Land, Svalbard, by geomorphic means. *Norsk Geografisk Tidsskrift—Norwegian Journal of Geography*, 56(2): 96–103.

Isarin, R.F.B., Renssen, H., & Vandenberghe, J. (1998) The impact of the North Atlantic Ocean on the Younger Dryas climate in northwestern and central Europe. *Journal of Quaternary Science*, 13(5): 447–453.

Kirkbride, M.P., & Deline, P. (2018) Spatial heterogeneity in the paraglacial response to post-Little Ice Age deglaciation of four headwater cirques in the Western Alps. *Land Degradation & Development*, 29(9): 3127–3140.

Knight, L., Boston, C.M., & Lovell, H. (2023) Glacial geomorphology in the Wicklow Mountains, Ireland. *Journal of Maps*, 19(1): 2132885.

Leira, M., Cole, E.E., & Mitchell, F.J.G. (2007) Peat erosion and atmospheric deposition impacts on an oligotrophic lake in eastern Ireland. *Journal of Paleolimnology*, 38: 49–71.

Lie, Ø., Dahl, S.O., & Nesje, A. (2003) A theoretical approach to glacier equilibrium-line altitudes using meteorological data and glacier mass-balance records from southern Norway. *The Holocene*, 13(3): 365–372.

Lifton, N., Sato, T., & Dunai, T.J. (2014) Scaling in situ cosmogenic nuclide production rates using analytical approximations to atmospheric cosmic-ray fluxes. *Earth and Planetary Science Letters*, 386: 149–160.

Lukas, S. (2006) Morphostratigraphic principles in glacier reconstruction-a perspective from the British Younger Dryas. *Progress in Physical Geography: Earth and Environment*, 30(6): 719–736.

Lukas, S., & Bradwell, T. (2010) Reconstruction of a Lateglacial (Younger Dryas) mountain ice field in Sutherland, northwestern Scotland, and its palaeoclimatic implications. *Journal of Quaternary Science*, 25(4): 567–580.

Lukas, S., Benn, D.I., Boston, C.M., Brook, M., Coray, S., Evans, D.J.A. et al. (2013) Clast shape analysis and clast transport paths in glacial environments: A critical review of methods and the role of lithology. *Earth-Science Reviews*, 121: 96–116.

Marrero, S.M., Phillips, F.M., Borchers, B., Lifton, N., Aumer, R., & Balco, G. (2016) Cosmogenic nuclide systematics and the CRONUScalc program. *Quaternary Geochronology*, 31: 160–187.

Matmon, A., Haeussler, P.J., & ASTER Team. (2020) Sediment sources and transport by the Kahiltna Glacier and other catchments along the south side of the Alaska Range, Alaska. *Geosphere*, 16(3): 787–805.

Menting, F., Langston, A.L., & Temme, A.J.A.M. (2015) Downstream fining, selective transport, and hillslope influence on channel bed sediment in mountain streams, Colorado Front Range. *Geomorphology*, 239: 91–105.

Mills, S.C, Grab, S.W, & Carr, S.J. (2009) Recognition and palaeoclimatic implications of late Quaternary niche glaciation in eastern Lesotho. *Journal of Quaternary Science*, 24(7): 647–663.

Mills, S.C., Le Brocq, A.M., Winter, K., Smith, M., Hillier, J., Ardakova, E. et al. (2019) Testing and application of a model for snow redistribution (Snow_Blow) in the Ellsworth Mountains, Antarctica. *Journal of Glaciology*, 65(254): 957–970.

Mitchell, W.A. (1996) Significance of snowblow in the generation of Loch Lomond Stadial (Younger Dryas) glaciers in the western Pennines, northern England. *Journal of Quaternary Science*, 11(3): 233–248.

Ohmura, A., & Boettcher, M. (2018) Climate on the equilibrium line altitudes of glaciers: theoretical background behind Ahlmann's P/T diagram. *Journal of Glaciology*, 64(245): 489–505.

Ohmura, A., Kasser, P., & Funk, M. (1992) Climate at the equilibrium line of glaciers. *Journal of Glaciology*, 38(130): 397–411.

Oien, R.P., Rea, B.R., Spagnolo, M., Barr, I.D., & Bingham, R.G. (2022) Testing the area–altitude balance ratio (AABR) and accumulation–area ratio (AAR) methods of calculating glacier equilibrium-line altitudes. *Journal of Glaciology*, 68(268): 357–368.

Olson, M., & Rupper, S. (2019) Impacts of topographic shading on direct solar radiation for valley glaciers in complex topography. *The Cryosphere*, 13(1): 29–40.

Pellitero, R., Rea, B.R., Spagnolo, M., Bakke, J., Hughes, P., Ivy-Ochs, S. et al. (2015) A GIS tool for automatic calculation of glacier equilibrium-line altitudes. *Computers & Geosciences*, 82: 55–62.

Rasmussen, S.O., Bigler, M., Blockley, S.P., Blunier, T., Buchardt, S.L., Clausen, H.B. et al. (2014) A stratigraphic framework for abrupt climatic changes during the Last Glacial period based on three synchronized Greenland ice-core records: refining and extending the INTIMATE event stratigraphy. *Quaternary Science Reviews*, 106: 14–28.

Rea, B.R. (2009) Defining modern day Area-Altitude Balance Ratios (AABRs) and their use in glacier-climate reconstructions. *Quaternary Science Reviews*, 28(3–4): 237–248.

Rea, B.R., & Evans, D.J.A. (2007) Quantifying climate and glacier mass balance in north Norway during the Younger Dryas. *Palaeogeography, Palaeoclimatology, Palaeoecology*, 246(2–4): 307–330.

Reimer, P.J., Austin, W.E.N., Bard, E., Bayliss, A., Bracewell, P.G., Bronk Ramsey, C. et al. (2020) The IntCal20 Northern Hemisphere radiocarbon age calibration curve (0–55 cal kBP). *Radiocarbon*, 62(4): 725–757.

Robertson, D.W. (1989) Aspects of the Lateglacial and Flandrian Environmental History of the Brecon Beacons, Fforest Fawr, Black Mountain and Abergavenny Black Mountains, South Wales (with Emphasis on the Lateglacial and Early Flandrian periods). Unpublished PhD Thesis, University of Wales.

Shakesby, R.A. (1989) Variability in Neoglacial moraine morphology and composition, Storbreen, Jotunheimen, Norway: within-moraine patterns and their implications. *Geografiska Annaler: Series A, Physical Geography*, 71(1–2): 17–29.

Sissons, J.B. (1980) Palaeoclimatic inferences from Loch Lomond advance glaciers. In *Studies in the Lateglacial of North West Europe*, Lowe, J.J., Gray, J.M., Robinson, D.E. (eds). Pergamon Press: Oxford; 31–43.

Sissons, J.B., & Sutherland, D.G. (1976) Climatic inferences from former glaciers in the south-east Grampian Highlands, Scotland. *Journal of Glaciology*, 17(76): 325–346.

Standell, MR. (2014) Late Glacial (Younger Dryas) Glaciers and Ice-Sheet Deglaciation in the Cairngorm Mountains, Scotland: Glacier Reconstructions and Their Palaeoclimatic Implications. Unpublished PhD thesis, Loughborough University.

Tomkins, M.D., Dortch, J.M., Hughes, P.D., Huck, J.J., Tonkin, T.N., & Barr, I.D. (2018) Timing of glacial retreat in the Wicklow Mountains, Ireland, conditioned by glacier size and topography. *Journal of Quaternary Science*, 33(6): 611–623.

Warren, W.P. (1993) *Wicklow in the Ice Age: An Introduction and Guide to the Glacial Geology of the Wicklow District*. Geological Survey of Ireland: Dublin.

Wilson, P. (2004) Evidence for and reconstruction of a Nahanagan Stade glacier at Croloughan Lough, Derryveagh mountains, Co. Donegal. *Irish Journal of Earth Sciences*, 22: 45–54.

Winkler, S. (2020). Terminal moraine formation processes and geomorphology of glacier forelands at the selected outlet glaciers of Jostedalsbreen, South Norway. In: Beylich, A.A. (Ed.) *Landscapes and Landforms of Norway*. Springer International Publishing: Cham; 33–69.

Winkler, S., & Matthews, J.A. (2010) Observations on terminal moraine-ridge formation during recent advances of southern Norwegian glaciers. *Geomorphology*, 116(1–2): 87–106.

Zhang, S., Li, X., & Chen, Y. (2015) Error assessment of grid-based direct solar radiation models. *International Journal of Geographical Information Science*, 29(10): 1782–1806.